Abstract

The source and thermal evolution history of organic matter for the Longmaxi shale are still debated. This study analyzed the molecular and stable carbon isotopic compositions of hydrocarbons (CH_4, C_2H_6, and C_3H_8) and CO_2 as well as the stable hydrogen isotopic compositions of methane, ethane, and noble gases (He, Ne, Ar, Kr, and Xe). Shale gases in the WY and CN areas show an extremely-low-wetness with CH_4 concentrations range from 93.41% to 99.01%. Non-hydrocarbon gases are mainly N_2 (0.22% - 2.81%) and CO_2 (0.03% - 1.35%). H_2S have not been detected. Different $\delta^{13}C_1$ and $\delta^{13}C_2$ values in WY and CN shale gases (WY: −37.3‰ to −35.0‰ and −40.3‰ to −38.3‰, CN: −29.8‰ to −26.3‰ and −35.3‰ to −32.7‰) and various carbon isotope-composition distribution patterns ($\delta^{13}C_1>\delta^{13}C_2<\delta^{13}C_3$ and $\delta^{13}C_1>\delta^{13}C_2>\delta^{13}C_3$) of hydrocarbons indicate a complex evolution process. WY shale gases include more oil-cracking gas than CN shale gases, suggesting WY shale gases more like come from Type I-II organic matter. In shale gas systems, methane content and $\delta^{13}C_1$ ratios vary with the degree of thermal evolution, so the origin of shale gas cannot be determined using carbon isotope data alone. The wide range of $\delta^{13}C_{CO2}$ values (−8.9‰ to −0.8‰) and $N_2/^{40}Ar$ ratios (20.8 to 165.1) suggests multiple origins of the gases. Emeishan mantle plume provides the source of heat for some thermo-genic gas. Noble gas isotopic compositions ($^3He/^4He$: 0.001Ra to 0.019Ra) indicate air and crustal origins with no significant contribution from the mantle. $^{40}Ar/^{36}Ar$ ratios (1194.3 - 4604.5) are consistent with the age of Longmaxi strata calculated by accumulative effect of Ar isotope. The shale gas humidity, carbon isotope ratios, and the carbon isotope-composition distribution patterns may contain information indicating the shale gas sweet spot.

Keyword: Stable Isotopic Compositions, Shale Gas, Noble Gas Isotopes, Sources, Evolution, Longmaxi Formation

1. Introduction

Shale gas resources in China are mainly distributed in Sichuan Basin. Changning (CN)-Weiyuan (WY) National Shale Gas Demonstration Zone (Fig. 1) is one of the primary and most productive shale gas plots in China due to the establishment of several substantial shale gas fields in this area (Dong *et al*., 2016; Zou *et al*., 2016). However, although extensive research on organic geochemistry characteristics (Tuo et al., 2016), pore evolution (Song et al., 2020), petrophysical characteristics (Yang et al., 2019; Liang et al., 2020), and tectonic evolution background (Zhou et al., 2014; Xiao et al., 2012) of shale in the Sichuan Basin, its origin and evolution have not been clearly clarified. For better understand the shale gas generation mechanism and guide the production of shale gas, the sources and evolution processes of the Longmaxi Formation shale gas needs in-depth research.

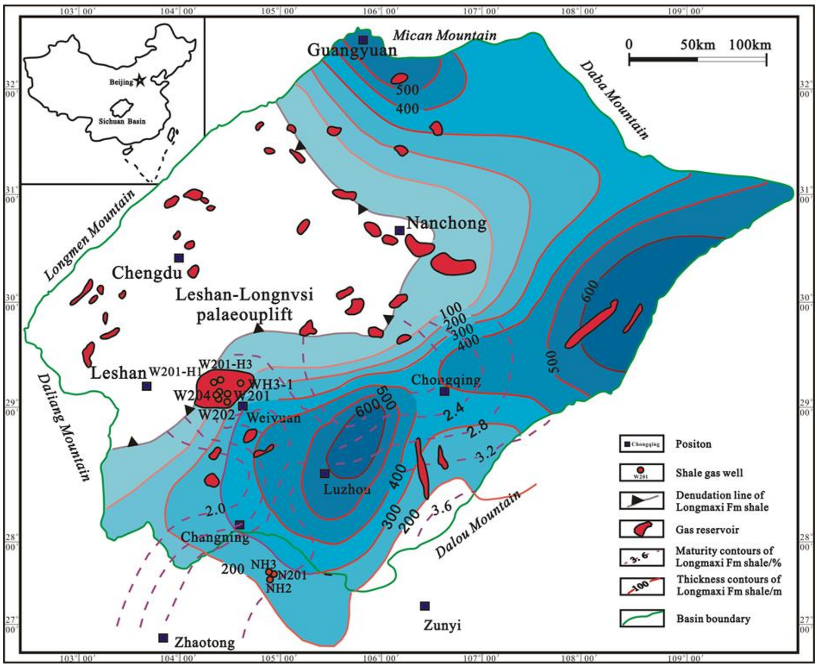

Fig. 1 *Geological map of the Sichuan Basin depicting the primary gas sampling sectors, the isolines of Ro values, and the shale thicknesses of the Longmaxi Formation, Sichuan Basin, China (after Zhang et al., 2018; Dai et al., 2014b).*

Shale gas is generated from self-contained, sealed petroleum systems, and exhibits many different gas geochemical characteristics compared to conventional natural gas (Tilley and Muehlenbachs, 2013, Hao and Zou, 2013, Gao *et al*., 2014). Recent works have reported that gas geochemical characteristics in shale gases from the same strata could vary in different regions (Cao *et al*., 2018; Zhang *et al*., 2018a). These differences reflect the complex histories of shale gas generation and associated isotopic fractionation as well as in-situ "mixing and accumulation" of gases generated from different precursors at different thermal maturities (Hao and Zou, 2013). During the generation and evolution process, the shale gas relative elemental abundance and isotopic compositions will continually change, due to the fractionation effect (Wang et al., 2015a; Xia et al., 2013). Being generated in a closed system and with little migration, shale gas has a more remarkable genetic accumulation effect than conventional natural gas (Hao and Zou, 2013; Behar et al., 1995). So, shale gas retains more original information about how oil and gas produced from source rocks, and their gas geochemical characteristics could reflect the evolution processes of fossil energy production in a closed system. Gas geochemistry characteristics of shale gas will help us to further understand the generation and evolution of natural gas system.

Gas geochemistry is widely used in shale-gas exploration and can provide an important medium with which to understand the evolution, migration, and accumulation of gases. It has been applied in the study of various gas systems by scholars worldwide (Zhou et al., 2019; Liu et al., 2019; Wang et al., 2017). To establish the origins of these natural gases, the stable carbon isotopes of methane, ethane, propane, and carbon dioxide, and stable hydrogen isotopes in methane, have been used (Zhang et al., 2018b; Rahayudin et al., 2020; Zou *et al*., 2007). Noble gases are also powerful tools with which to determine the details of the evolution of natural gas systems, due to their scarcity, inertness, and distinct isotopic composition in three major sources, including the atmosphere (e.g., $^{3}He/^{4}He=1.4\times10^{-6}$, $^{40}Ar/^{36}Ar=296$), mantle (e.g., $^{3}He/^{4}He\geqslant1\times10^{-5}$, $^{40}Ar/^{36}Ar\geqslant10{,}000$), and crust (e.g., $^{3}He/^{4}He\leqslant1\times10^{-7}$, $^{40}Ar/^{36}Ar\geqslant5{,}000$) (Porcelli and Ballentine, 2002, and citations within). The present study is aimed at determining the origins and evolution of Longmaxi shale gas by investigating the molecular and stable carbon isotopic compositions of gaseous hydrocarbons (CH_4, C_2H_6, and C_3H_8) and CO_2, the stable hydrogen isotopic compositions of methane, and noble gas isotopic compositions (He, Ne, Ar, Kr, and Xe). In order to constrain the source of Longmaxi shale gas and determine its evolutionary history, shale gas samples collected from 19 shale gas wellheads in the WY and CN blocks were analyzed, and these shale gas components and stable isotopic composition data sets were analyzed. Comparisons were made with geochemical data from China 's recently released WY, CN, and FL shale gas and the US Barnette and Fayetteville shale gas.

2. Geological setting

The Sichuan Basin covers an area of more than 1.8×10^{5} km^{2} and is located at the west of the Yangtze Craton, Southeast China (Fig. 1). It is structurally complex, superimposed basin, confined on the north by Daba Mountain (uplift) and Micang Mountain (fold belt), on the south by Daliang Mountain (fold belt), on the west by Longmen Mountain (fold belt) and on the east by Dalou Mountain (Fig. 1). The Sichuan Basin lies in the transition zone between the Palaeo-Pacific and Tethys-Himalayan tectonic areas (Liu *et al*., 2016). It underwent two major tectonic evolution stages, *i.e*., an earlier Palaeozoic Period cratonic depression and a later foreland basin stage in the Triassic (Xu *et al*., 2018; see Fig. 2). The effects of the Caledonian, Hercynian, Indosinian, and Yanshanian orogenies in addition to the Himalayan movement produced complicated deforming and denuding within the basin's deposition (Fig. 2; Zhu *et al*., 2010a, 2010b; Chen *et al*., 2014). At the end of the Middle Triassic, the Sichuan Basin experienced a transition from marine to continental sedimentation. Six sets of source rocks have been identified in the Lower Cambrian, Lower Silurian, Lower Permian, Upper Permian, Upper Triassic, and Lower Jurassic formations, of which the first 4 sets are considered major basin source rocks (Huang *et al*., 1997; Zhu *et al*., 2007; Figs. 1 and 2). However, intensive tectonic movements, specifically those observed throughout the Caledonian, Yanshanian, Indosinian, and Himalayan orogenies (Wei *et al*., 2008; Hao and Zou, *et al*., 2013; Liu *et al*., 2016), produced many faults and unconformity surfaces. These have resulted in various hydrocarbon-migration and gas-preservation mechanisms.

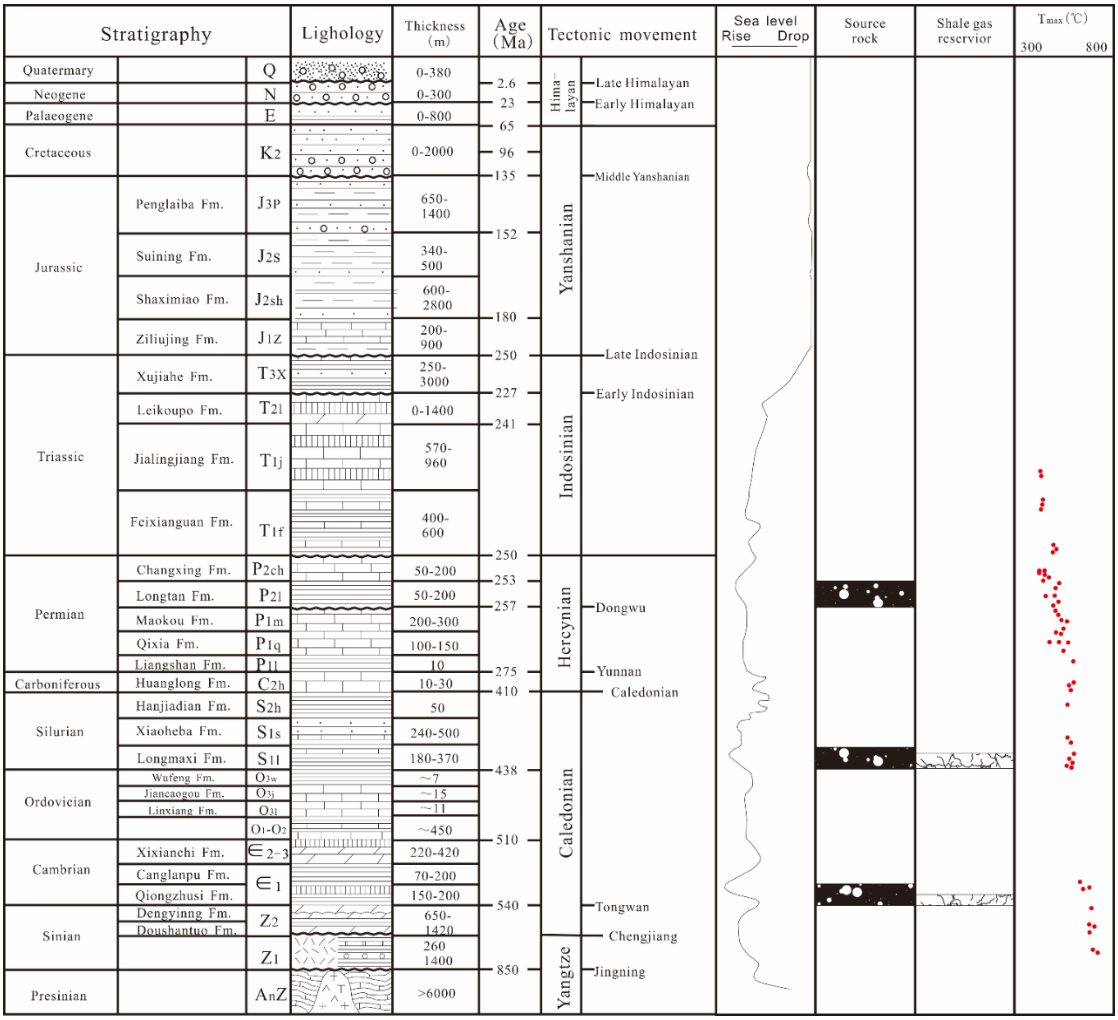

Fig. 2 *Schematic stratigraphy system of the Sichuan Basin, and the sedimentary environments and main tectonic occurrences (modified from Zou et al. 2015; Dai et al. 2014b; Chen et al. 2014; Liang et al. 2009).*

The basement of Sichuan Basin is composed of Middle-Upper Proterozoic metamorphic and magmatic rocks. Lower Paleozoic marine organic-rich black shale strata are widespread in Sichuan Basin. The primitive organic matter belongs to type-I and/or -II_1 kerogens (Dai *et al.*, 2016). In the Cambrian and Silurian shales, the comparable vitrinite reflectance (EqVRo, %) values range from 1.8–3.8% (Zou *et al.*, 2016; Guo, 2016), indicating that they are chiefly thermally over-mature and within a dry-gas-generation state (Wang *et al.*, 2013; Dai *et al.*, 2016). Longmaxi Formation black shale is one of the most important strata owing to its significantly large thickness and wide distribution. However, while present in CN area, they are missing in the northwestern part of the WY area. The Longmaxi Formation is consisted of black graptolitic shale in its nether section and nodular limestone in its higher section (Figs. 1 and 2; Zhao *et al.*, 2006).

The WY shale gas area is located on the southeastern edge of the Leshan-Longnvsi paleo-uplift (Fig. 1). There are no Devonian and Carboniferous strata and not exhibit well-developed Ordovician strata due to Hercynian orogeny. The Yanshan and Himalayan orogeny resulted in complete erosion of the Jurassic and early Cretaceous strata. Dengying Formation is the main conventional gas reservoir in this region (Dai, 2003; Wei *et al.*, 2008). Lower Cambrian Jiulaodong Formation shale and the Lower Silurian Longmaxi Formation shale are the main organic-rich shale developed in the Lower Paleozoic strata in the Weiyuan area. The two sets of shales are mainly type I and highly matured (Huang *et al.*, 2012).

CN shale gas area lies in the border of the southern fold belt in the southern Sichuan Basin and the Daloushan Fault-fold Zone. It is limited to the Lianhuasi-Laowengchang structure to the north, the Baiyanglin-Dazhai anticline structure to the south, the Jiacunxi structure to the west, and faces the Gaomuding structure across the Phoenix Mountain syncline to the east. From bottom to top, the Ordovician Wufeng, Silurian Longmaxi, Carboniferous Huanglong, and Permian Longtan formations are developed. In the CN structure, the oldest strata outcropped is Lower Cambrian Longwangmiao Formation. The Lower Silurian Longmaxi Formation in the CN area consists of a set of shallow-marine clastic rock (Liang *et al.*, 2009).

3. Samples and experiments

3.1 Shale gas specimens

All gas samples were collected directly from producing wellheads in high-pressure cylinders (maximum pressure capacity 15 MPa, volume 1000 mL), with metal valves on both ends. The cylinders were heated at 150°C under vacuum and then pumped to vacuum pressure (~10^{-2} Pa) in the laboratory before being shipped to the field. Atmospheric contamination during sampling was minimized by allowing the gas to flush through the lines and cylinders for approximately 10 - 15 mins, during which the cylinder valves were shut and opened several times (Gonzalez-Penagos *et al.*, 2016; Cao *et al.*, 2016, 2018). After the completion of sample collection, the cylinder was tested for leaks underwater. The location details of the sampling areas are revealed in Fig. 1.

3.2 Analytical procedure

Molecular composition and stable carbon, hydrogen, and noble gas isotopic compositions were analyzed in the Key Laboratory of Petroleum Resources Research, Institute of Geology and Geophysics, Chinese Academy of Sciences (Lanzhou, China). The non-hydrocarbon molecular composition (CH_4, CO_2, O_2, H_2, H_2S, N_2, He, and Ar) analyses were performed using a MAT 271 mass spectrometer (Cao *et al*., 2016). The hydrocarbon (CH_4, C_2H_6, and C_3H_8) abundances were examined with an Agilent 6890N gas chromatograph (GC) equipped with a flame-ionization detector (FID). A capillary column (PLOT Al_2O_3, 50 m × 0.53 mm) was utilized to divide the individual hydrocarbon gas components (C_1–C_3). The GC oven temperature was initially placed at 30ºC for 10 min and ramped up to 180ºC at a rate of 10ºC/min and kept at 180ºC for 20–30 min (Cao *et al*., 2018; Zhang *et al*., 2018a; Dai *et al*., 2014b).

A Finnigan MAT Delta Plus XP mass spectrometer interfaced to an HP 6890 GC was employed to determine stable carbon isotope ratios. Individual hydrocarbon components (C_1–C_3) and CO_2 were divided on an HP-PLOT column (30 m×0.32 mm) with He as the carrier gas (2 mL/min). The GC oven temperature was elevated from an initial temperature of 35ºC to 80ºC at a rate of 8 ºC/min, and then to 260ºC at a rate of 5ºC/min, at which it was maintained for 10 min. Individual compounds were oxidized at 940ºC via an oxidation ceramic microreactor loaded with twisted wires (NiO/CuO/Pt). The high-temperature oxidation furnace was then used to oxidize the hydrocarbons into CO_2, which was examined using a DeltaPlus XP carbon isotope mass spectrometer. The average reproducibility was better than ±0.5‰ (*n*=6) for inter-laboratory standards. The stable carbon isotope-ratio ($\delta^{13}C$) values are documented in "δ" notation in per mill (‰), respective of V-PDB (Vienna Pee Dee Belemnite) (Li *et al*., 2014; Dai *et al*., 2014b).

Stable hydrogen isotope ratios were measured by MAT-253 isotope mass spectrometer (Thermo Fisher Scientific) also equipped with an HP6890 gas chromatograph. Methane and ethane were separated chromatographically on a fused silica capillary column (HP-PLOT Q, 30 m × 0.32 mm × 20 µm). The initial temperature of GC oven was kept at 40ºC for 5 min, then elevated from 40°C to 80ºC at a rate of 5 ºC/min, from 80°C to 140ºC at a rate of 10ºC/min, and finally from 140°C to 260ºC at a rate of 30ºC/min. The pyrolysis-oven temperature was 1450ºC (Dai *et al*., 2014b) and standard H_2 was utilized as the reference gas. The analytical precision approximated to be ±3‰. The stable-hydrogen-isotope information is reported in δ notation (δ^2H, ‰) relative to Vienna Standard Mean Ocean Water (VSMOW=0.0‰) and the inter-laboratory standard were used together to calibrate the hydrogen isotope.

Noble gas isotopic composition was measured using a specially designed noble gas mass spectrometry system (Cao *et al*., 2016, 2018). The high-pressure sample cylinder was connected to a purification line with connecting fittings (Swagelok). Then, part of the gas was introduced into a gas pipette (8.5 cm^3), and then pressure and temperature of the gas were measured to calculate the absolute gas amount. Next, a 1.5 cm^3 volume of gas was introduced into the noble gas purification line, where these gases were purified by exposing them to a titanium sponge heated to 800 ºC.

Majority of active gases (C_1 - C_4, H_2O, O_2, N_2, and CO_2, etc.) can be removed. H_2 in the gas can be eliminated by Zr-Al getters running at room temperature. Purified noble gases were separated by a cryogenic trap (8 - 475 K) filled with activated charcoal. He, Ne, Ar, Kr, and Xe were released for analysis at the cryogenic trap temperature of 15K, 50K, 100K, 150K and 230K, respectively. The details of analytical procedure were described in Cao et al. (2018). ^{4}He, ^{20}Ne, ^{22}Ne ^{40}Ar, and ^{36}Ar were examined with a Faraday collector, and ^{3}He, ^{21}Ne, ^{38}Ar, Kr, and Xe isotopes were analyzed with an electron multiplier. The atmospheric standard (collected from the top of Gaolan Mountain in Lanzhou) was measured before and after each sample. Interference from $(^{40}Ar)^{2+}$ and $(^{12}C^{16}O_2)^{2+}$ on $(^{20}Ne)^{+}$ and $(^{22}Ne)^{+}$ was also corrected (Ye *et al*. 2007, Zhang *et al*., 2013).

4. Results

4.1 Chemical compositions

The shale gases from WY and CN are mainly comprised of CH_4 (93.41%–99.00%) with minor amounts of C_2H_6 (0.28%–0.50%) and non-hydrocarbon gases

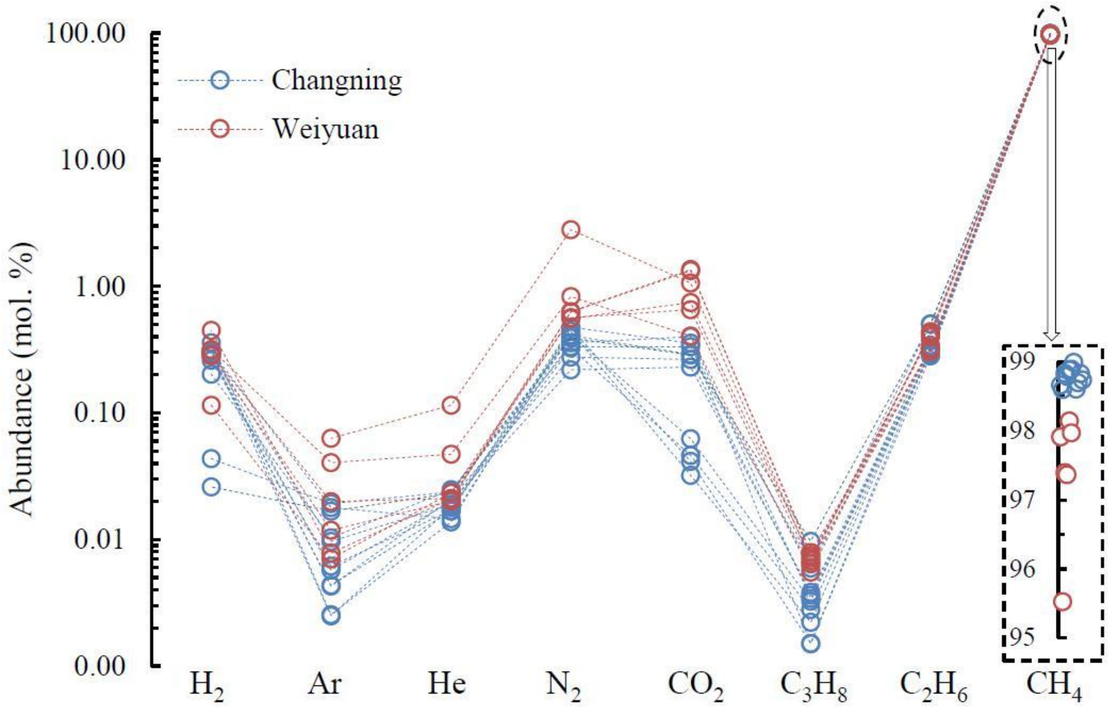

Fig. 3 *Distribution of chemical composition in Longmaxi shale gas from the Weiyuan and Changning sectors of Sichuan Basin, China.*

(see Table 1), and it is one of the driest shale gases in the world (Dai *et al*., 2014a). The methane content in WY shale gas (average 97.39%) is slightly lower than that in CN shale gas (average 98.32%) (Table 1 and Fig. 3). The ethane and propane contents are lower than those observed in the Jiaoshiba shale gases from the Sichuan Basin eastern margin (Liu, 2016), from Fayetteville (Zumberge *et al*., 2012), and from the

Barnett shale gases, which were collected from the USA (Rodriguez and Philp, 2010). Non-hydrocarbon gases in WY and CN shale gases mainly consist of N_2 (0.22%–2.81%), CO_2 (0.03%–1.35%), and trace amounts of He (0.01%–0.12%) and Ar (0.002%–0.063%) (Table 1); H_2S was not been detected. The contents of CO_2 (average 0.92%) and N_2 (average 1.00%) in the WY area are higher than those in the CN area (averages of 0.19% and 0.37%, respectively) (Table 1 and Fig. 3).

Table 1 *Chemical composition (%) of Silurian Longmaxi shale gases in Weiyuan and Changning areas, Sichuan Basin, China.*

Gas field /area	Well	Depth (m)	Chemical Composition (%)								
			CH_4	C_2H_6	C_3H_8	CO_2	N_2	He	Ar	Ne	H_2
Changning	N201	1520-1523	98.67	0.42	0.01	0.33	0.33	0.02	0.010	-	0.20
	NH2-1	2790-4140	98.60	0.28	0.00	0.36	0.47	0.02	0.006	-	0.26
	NH2-2*	2322	93.41	0.28	0.00	0.08	0.30	0.02	0.01	-	-
	NH2-3	2453-3457	98.84	0.30	0.00	0.26	0.28	0.02	0.004	0.001	0.29
	NH2-5	-	98.79	0.32	0.00	0.04	0.47	0.01	0.003	0.025	0.36
	NH2-6	2448	98.89	0.33	0.00	0.23	0.22	0.02	0.006	0.002	0.31
	NH2-7	-	98.90	0.32	0.00	0.03	0.44	0.02	0.004	-	0.28
	NH3-1	2873-3973	99.00	0.30	0.00	0.05	0.33	0.02	0.002	0.002	0.30
	NH3-2	2738-3837.8	98.61	0.29	0.00	0.40	0.36	0.02	0.010	-	0.31
	NH3-3*	2650-3750	98.23	0.34	0.00	0.07	0.36	0.02	0.01	-	0.97
	NH3-4	2865-4545	98.70	0.50	0.01	0.29	0.41	0.02	0.019	-	0.04
	NH3-5	2700-4520	98.84	0.34	0.00	0.06	0.41	0.01	0.018	0.015	0.31
	NH3-6	2930-4481	98.74	0.50	0.01	0.29	0.39	0.02	0.017	0.003	0.03
Weiyuan	W201	1523	97.92	0.44	0.01	0.41	0.83	0.05	0.040	-	0.32
	W201-H3	2952-3609	95.53	0.42	0.01	1.06	2.81	0.12	0.063	0.039	0.00
	W204H1-2	4702	97.40	0.32	0.01	1.33	0.62	0.02	0.012	0.001	0.28
	W204H1-3	4702	97.37	0.31	0.01	1.35	0.63	0.02	0.020	-	0.29
	WH3-1	-	98.15	0.40	0.01	0.74	0.56	0.02	0.007	-	0.11
	W204	-	97.97	0.33	0.01	0.65	0.56	0.02	0.008	-	0.45

"*" Data from Zhang et al., 2018

4.2 Carbon- and hydrogen-isotope compositions

The $\delta^{13}C_1$ values of Longmaxi shale gases in WY area range from −37.3‰ to −35.0‰, the $\delta^{13}C_2$ values range from −40.3‰ to −38.3‰, and the $\delta^{13}C_3$ values range from −37.5‰ to −33.6‰. The shale gases from Longmaxi Formation in CN have heavier $\delta^{13}C_1$ (−29.8‰ to −26.3‰) and $\delta^{13}C_2$ (−35.3‰ to −32.7‰) values, and they are almost 8‰ and 5‰ heavier for $\delta^{13}C_1$ and $\delta^{13}C_2$, respectively than those in WY area. The $\delta^{13}C_3$ values span from −38.0‰ to −34.7‰ in CN area (Table 2). Shale gases from Longmaxi Formation in WY and CN areas both show reversal distribution patterns of carbon isotopic compositions from CH_4 to C_3H_8. CN shale gases show full carbon isotopic reversal, i.e., $\delta^{13}C_1 > \delta^{13}C_2 > \delta^{13}C_3$ (Table 2, Fig. 4(a), and Fig. 5). However, WY shale gases present two kinds of carbon isotopic reversal patterns, i.e., $\delta^{13}C_1 > \delta^{13}C_2 < \delta^{13}C_3$ and $\delta^{13}C_1 > \delta^{13}C_2 > \delta^{13}C_3$ (Table 2, Fig. 4(b), and Fig. 5).

Table 2 *Carbon (‰, V-PDB) and hydrogen (‰, V-SMOW) isotopic composition of shale gases from Silurian Longmaxi Formation shale in Weiyuan and Changning areas, Sichuan Basin, China.*

Gas field/area	Well	$\delta^{13}C$(VPDB)				δD (‰VSMOW)	
		$\delta^{13}C_{CO2}$	$\delta^{13}C_{C1}$	$\delta^{13}C_{C2}$	$\delta^{13}C_{C3}$	δD_1	δD_2
Changing	N201	-6.2	-28.9	-34.9	-36.7	-146.5	-152.0
	NH2-1	-4.0	-27.9	-35.0	-35.6	-141.5	-168.6
	NH2-2*	-4.8	-27.2	-34.2	-	-	-
	NH2-3	-8.9	-28.3	-35.3	-38.0	-148.0	-170.2
	NH2-5	-7.1	-26.3	-33.8	-37.0	-139.2	-163.0
	NH2-6	-3.2	-27.2	-34.2	-37.3	-148.2	-151.3
	NH2-7	-8.4	-27.6	-34.4	-35.9	-140.7	-168.2
	NH3-1	-3.8	-27.7	-34.4	-36.5	-149.2	-145.9
	NH3-2	-0.8	-27.3	-34.8	-34.7	-140.5	-135.2
	NH3-3*	-4.5	-29.3	-34.7	-37.2	-148.6	-165.2
	NH3-4	-	-27.2	-32.7	-	-139.3	-122.1
	NH3-5	-4.3	-28.9	-33.7	-34.9	-142.2	-161.6
	NH3-6	-4.1	-29.8	-34.9	-35.3	-144.6	-175.4
Weiyuan	W201	-7.3	-37.3	-38.3	-33.6	-138.7	-155.7
	W201-H3	-5.8	-35.3	-40.3	-37.5	-138.4	-150.3
	W204	-5.0	-35.0	-38.7	-	-138.2	-145.4
	W204H1-2	-2.2	-35.4	-39.0	-	-143.7	-151.9
	W204H1-3	-2.2	-35.2	-38.3	-	-147.0	-155.7
	WH3-1	-	-35.6	-40.3	-	-141.6	-144.2

"*" Data from Zhang et al., 2018

The $\delta^{13}C_{CO2}$ values of Longmaxi shale gases vary from −8.9‰ to −0.8‰ and are in the same range as that of Fuling (Yang *et al*., 2017; Xu *et al*., 2018) and Barnett shale gases (Zumberge *et al*., 2012; Rodriguez and Philp, 2010). However, they are heavier than those in most Fayetteville shale gases (Zumberge *et al*., 2012). The δD_1 and δD_2 values of Longmaxi shale gases in the CN area range from −149.2‰ to −139.2‰ and from −175.4‰ to −122.1%, respectively. These two values in the WY area are −147.0‰ to −138.2‰ and −155.7‰ to −144.2‰, respectively. Shale gases from most wells show a reversal distribution pattern for hydrogen isotopic composition ($\delta D_1 > \delta D_2$) in both the WY and CN areas (Table 2).

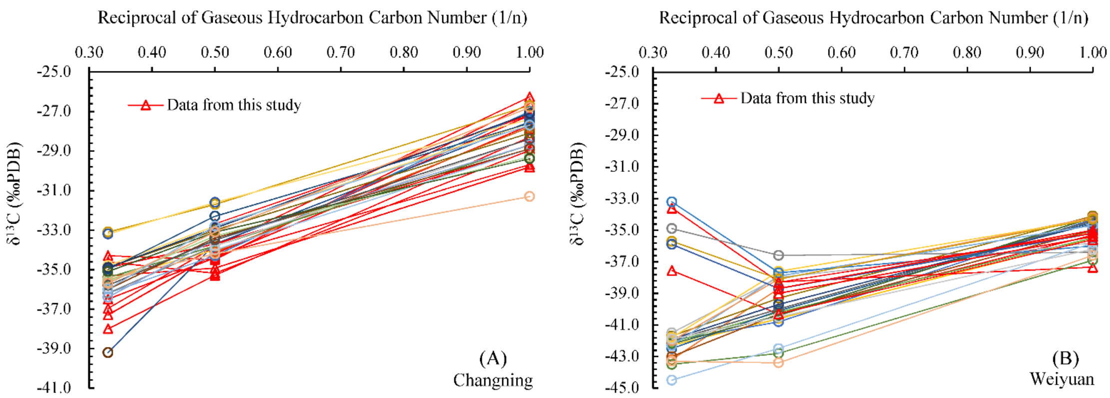

***Fig. 4** Relationship between $\delta^{13}C_n$ and reciprocal of carbon number (1/n) of (A) Changning and (B) Weiyuan shale gases, Sichuan Basin, China (data sources: Xu et al., 2018; Zhang et al., 2018; Yang et al., 2017; Feng et al., 2016, 2018; Dai et al., 2016; this study).*

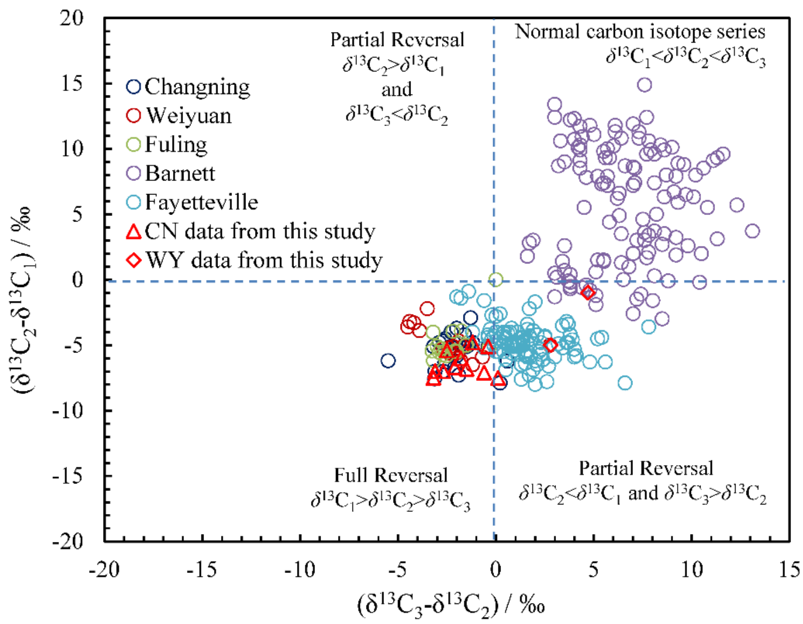

***Fig. 5** Variation of $\delta^{13}C_3$ - $\delta^{13}C_2$ as a function of $\delta^{13}C_2$ - $\delta^{13}C_1$ for gases in the Weiyuan, Changning, and Fuling shales in China, and from Barnett and Fayetteville shales in the USA, showing isotope dispersion patterns of methane, ethane, and propane (data sources: Xu et al., 2018; Zhang et al., 2018; Yang et al., 2017; Feng et al., 2016, 2018; Dai et al., 2016; Zumberge et al., 2012; this study).*

4.3 Noble-gas-isotope compositions

Noble gases (He, Ne, Ar, Kr, and Xe) are chemically inert and are not impacted by secondary chemical processes (chemical reactions or microbial functions) (Ozima and Podosek, 2002; Moreira, 2013). They have been proved to be the ideal natural tracers for studying the origin and evolution of fluids in sedimentary basins (Hilton *et al*., 2003; Warner *et al*., 2013). Noble gases combined with carbon and hydrogen isotopes have been applied to various natural gas studies previously (Kotarba *et al*., 2008, 2014; Schlegel *et al*., 2011).

Noble gas results for Longmaxi shale gases in WY and CN areas are presented in Table 3. The $^{3}He/^{4}He$ ratios of the samples are between 0.001 and 0.019 Ra (Ra is the atmospheric value of 1.4×10^{-6}), which were consistent with the average value of the crust-derived helium ratio, *i.e.*, 0.02 Ra (Ballentine and Burnard, 2002). The $^{20}Ne/^{22}Ne$ ratios were slightly higher than the atmospheric neon value (9.80, Allegre *et al*., 1987; Sarda *et al*., 1988) and lower than the mantle value (12.2, Ballentine et al., 2005). The $^{21}Ne/^{22}Ne$ ratios (0.006–0.047) of the Longmaxi shale gases vary from those of the atmosphere (0.029) and the crust (0.03–0.70) (Sarda *et al*., 1988; Ozima and Podosek, 2002), and were significantly reduced compared to that of nucleogenic Ne (0.3) (Ozima and Podosek, 2002). The $^{40}Ar/^{36}Ar$ ratios (1194.3-4604.5) are higher than that in air (295.5, Allegre et al., 1987, Lee et al., 2006) but much lower than the MORB values, which are often up to 10,000 and sometimes are as high as 44,000 (Burnard et al., 1997, Moreira et al., 1998). The $^{38}Ar/^{36}Ar$ values are close to that in the atmosphere (0.188), while the measured $^{4}He/^{20}Ne$ ratios (6611.2–67111.8) are much greater than the atmospheric ratio of 0.288, similar to recorded data for conventional natural gases (Zhou *et al*., 2005; Kotarba *et al*., 2008, 2014; Darrah *et al*., 2014). This indicates that there are no apparently atmosphere-derived noble gas contributions during sample collection and analysis.

Isotopic compositions of Kr and Xe in Longmaxi shale gases are the same as those in the air (Table 3). Krypton isotope ratios are between 0.197 and 0.253 (average 0.213), 0.185 and 0.210 (average 0.201), and 0.280 and 0.328 (average 0.300) for $^{82}Kr/^{84}Kr$, $^{83}Kr/^{84}Kr$, and $^{86}Kr/^{84}K$, respectively. $^{129}Xe/^{132}Xe$ ratios range from 0.917 to 1.364 (average 1.057) and $^{131}Xe/^{132}Xe$ values from 0.581 to 1.070 (average 0.808).

Table 3 *Isotopic compositions of noble gases (He, Ne, Ar, Kr and Xe) from Silurian Longmaxi Formation shale in Weiyuan and Changning areas, Sichuan Basin, China.*

Well	$^{3}He/^{4}He$	err(1σ)	$^{20}Ne/^{22}Ne$	err(1σ)	$^{21}Ne/^{22}Ne$	err(1σ)	$^{40}Ar/^{36}Ar$	err(1σ)	$^{38}Ar/^{36}Ar$	err(1σ)	$^{82}Kr/^{84}Kr$	err(1σ)	$^{83}Kr/^{84}Kr$	err(1σ)	$^{86}Kr/^{84}Kr$	err(1σ)	$^{129}Xe/^{132}Xe$	err(1σ)	$^{131}Xe/^{132}Xe$	err(1σ)	$^{4}He/^{20}Ne$
N201	1.6E-08	4.5E-09	9.9	0.7	0.037	0.009	1983.1	4.9	0.188	0.001	0.204	0.004	0.200	0.004	0.295	0.005	0.970	0.039	0.802	0.031	35206.9
NH2-1	1.8E-09	5.6E-09	8.9	0.5	0.029	0.008	1728.2	9.8	0.196	0.003	0.253	0.013	0.203	0.010	0.295	0.014	1.195	0.200	0.788	0.150	13034.2
NH2-2	1.3E-08	3.2E-09	-	-	-	-	1782.3	5.2	0.186	0.001	0.221	0.004	0.201	0.005	0.297	0.007	0.985	0.044	0.814	0.039	13890.1
NH2-3	3.0E-09	5.6E-09	9.7	0.4	0.022	0.005	1709.1	10.0	0.194	0.003	0.221	0.011	0.205	0.010	0.328	0.013	1.332	0.360	0.887	0.290	18106.3
NH2-5	9.6E-07	1.4E-07	9.2	0.6	0.036	0.007	1497.1	7.3	0.189	0.003	0.202	0.008	0.206	0.010	0.313	0.013	1.164	0.150	0.772	0.120	8759.4
NH2-6	6.3E-09	5.1E-09	-	-	-	-	1567.9	11.0	0.199	0.003	0.205	0.011	0.191	0.009	0.285	0.012	1.364	0.230	1.070	0.210	6611.2
NH2-7	6.2E-09	2.3E-09	10.8	0.4	0.032	0.005	1760.0	4.6	0.185	0.001	0.211	0.005	0.203	0.004	0.304	0.005	1.001	0.040	0.860	0.034	21099.2
NH3-1	1.4E-08	5.4E-09	10.0	0.5	0.032	0.009	1733.2	4.2	0.186	0.001	0.207	0.005	0.204	0.005	0.307	0.006	1.023	0.036	0.796	0.029	31242.7
NH3-2	1.1E-08	3.4E-09	9.8	0.4	0.035	0.006	1647.8	4.5	0.183	0.001	0.215	0.005	0.208	0.005	0.301	0.007	0.961	0.047	0.721	0.041	22321.5
NH3-3	2.9E-09	3.3E-09	11.7	0.5	0.036	0.006	1590.9	3.3	0.189	0.001	0.218	0.004	0.197	0.004	0.297	0.005	0.967	0.035	0.768	0.029	17976.2
NH3-4	1.2E-08	3.3E-09	10.4	0.4	0.021	0.007	1733.5	3.9	0.184	0.001	0.209	0.005	0.210	0.005	0.293	0.008	1.012	0.038	0.809	0.034	27166.6
NH3-5	7.0E-09	2.7E-09	-	-	-	-	1194.3	3.6	0.178	0.001	0.203	0.002	0.204	0.002	0.302	0.003	0.990	0.022	0.753	0.018	-
NH3-6	1.1E-08	4.2E-09	11.1	0.8	0.047	0.007	1666.1	4.9	0.184	0.001	0.208	0.005	0.204	0.005	0.296	0.006	1.076	0.063	0.869	0.043	23293.5
W201	1.4E-08	3.2E-09	10.3	0.3	0.040	0.008	1838.2	5.7	0.192	0.002	0.213	0.004	0.200	0.003	0.303	0.010	0.917	0.056	0.900	0.038	18267.8
W201-H3	1.6E-08	2.1E-09	10.0	0.3	0.006	0.006	4604.5	8.7	0.204	0.001	0.216	0.003	0.205	0.003	0.302	0.003	1.104	0.112	0.857	0.042	67111.8
W204	1.2E-08	6.2E-09	9.0	0.7	0.032	0.009	1496.9	5.3	0.186	0.002	0.212	0.007	0.190	0.007	0.295	0.011	1.086	0.130	0.831	0.095	15345.5
W204H1-2	1.0E-09	7.6E-09	11.7	0.7	0.015	0.007	1446.5	7.0	0.192	0.002	0.210	0.007	0.197	0.008	0.302	0.009	0.980	0.093	0.581	0.070	7901.1
W204H1-3	8.1E-09	1.1E-08	9.5	0.5	0.031	0.008	1444.3	5.1	0.192	0.002	0.222	0.008	0.198	0.008	0.298	0.010	1.002	0.095	0.692	0.082	9299.5
WH3-1	1.7E-08	8.3E-09	9.6	0.5	0.024	0.009	1441.5	3.8	0.188	0.002	0.197	0.007	0.185	0.006	0.280	0.009	1.013	0.086	0.801	0.075	12206.0
Air*	1.4E-06	-	9.8	-	0.029	-	295.5	-	0.188	-	0.202	-	0.201	-	0.305	-	0.983	-	0.789	-	0.318

"*" Data from Ozima and Podosek, 2002

5. Discussion

5.1 Sources and evolution of hydrocarbons

Shale gas is a self-contained, self-storage, and self-enclosed system. To identify the sources of shale gas is the basis and guarantee of investigating the evolution of shale gas. Previous studies suggest that the Longmaxi Formation shale is Type I-II organic matter (Zou *et al*., 2015, 2016). Dai et al. (2014a) proposed a gas-classification system that uses a three-isotope plot of $\delta^{13}C_1$-$\delta^{13}C_2$-$\delta^{13}C_3$ (Fig. 6), in which carbon isotope values of Longmaxi Formation shale gas in the WY and CN areas are near or within Zone III, suggesting an isotopic reversal zone. Moreover, it seems that these hydrocarbons are from terrestrial humic source rock (Fig. 7), which is not consistent with the specific source of Type I-II organic matter. This contradiction may result from the combination of kerogen-and oil-cracking gases, which can modify the carbon isotopic composition of shale gas (Tian *et al*., 2006, 2007; Hao *et al*., 2008). Natural methane from various genetic types can be more easily differentiated on a δD_1-$\delta^{13}C_1$ plot than they can by using carbon isotope ratios alone (Schoell *et al*., 1980). WY and CN shale gases belong to thermogenic natural gas (Dai *et al*., 2014b). Figure 7 shows that CN shale gases are in the Type-II kerogens area, while WY shale gases fall into the Type-III kerogens. An apparent difference of carbon and hydrogen isotopic composition of Longmaxi Formation shale gases exist in the WY and CN areas, which has been reported in previous work as well (Dai *et al*., 2014b; Cao *et al*., 2016, Zhang *et al*., 2018a). This indicates that the sources of hydrocarbons in WY and CN are different or their evolution is not absolutely the same although they are all in the same strata.

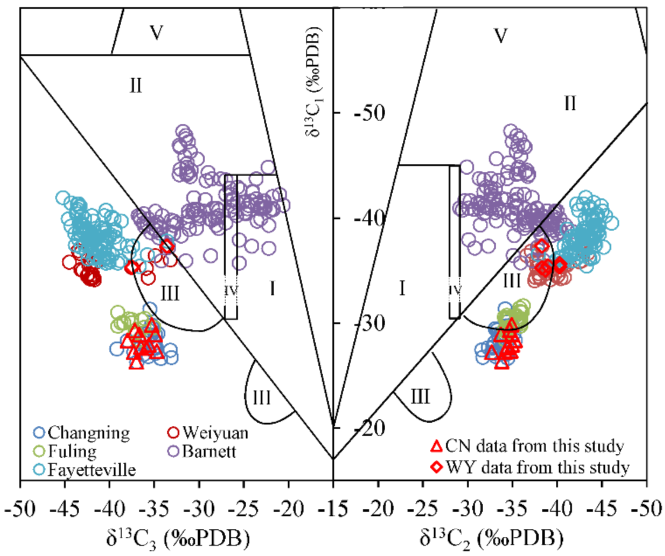

Fig. 6 *Plot of Longmaxi Formation shale gas $\delta^{13}C_1$-$\delta^{13}C_2$-$\delta^{13}C_3$ identification in the Weiyuan and Changning sectors of the Sichuan Basin, China (data sources: Xu et al., 2018; Zhang et*

al., 2018; Yang et al., 2017; Feng et al., 2016, 2018; Dai et al., 2016; Zumberge et al., 2012; this study). I, coal-derived gas; II, oil-associated gas; III, mixed gas with carbon-isotope reversal; IV, coal-derived gas and/or oil-associated gas; V, microbial gas.

The evolution of hydrocarbon can change the carbon isotopic composition of shale gases, especially in a sealed system. Moreover, detailed and in-depth evolution information can help us to recognize the real source rock. Based on the relationship among $\delta^{13}C_1$, $\delta^{13}C_2$, and $\delta^{13}C_3$, four types of isotope- distribution patterns can be identified: normal series ($\delta^{13}C_1<\delta^{13}C_2<\delta^{13}C_3$), partial reversal I ($\delta^{13}C_2<\delta^{13}C_1$ and $\delta^{13}C_2< \delta^{13}C_3$), partial reversal II ($\delta^{13}C_2>\delta^{13}C_1$ and $\delta^{13}C_2>\delta^{13}C_3$), and complete reversal ($\delta^{13}C_1>\delta^{13}C_2>\delta^{13}C_3$) (Fig. 5). Carbon isotopic composition of Longmaxi Formation shale gas in the WY and CN regions exhibit partial reversal I and complete reversal distribution patterns. However, most Barnett shale gases exhibit a normal carbon isotope distribution, whereas most Fayetteville shale gases display a partial reversal II distribution pattern (Fig. 5). WY, CN, and FL shale gases present the highest thermal evolution (Ro=2.0%–4.5%), while Barnett and Fayetteville shale gases have Ro values of 0.6% and 1.6%, respectively (Jiang *et al.*, 2008). Carbon isotopic composition of shale gas could change with thermal evolution (Hao and Zou, 2013; Dai *et al.*, 2014b) [Fig. 8(b)], therefore, it may be one of the causes of the different carbon isotope distributions of WY, CN, Fuling, Barnett, and Fayetteville shale gases.

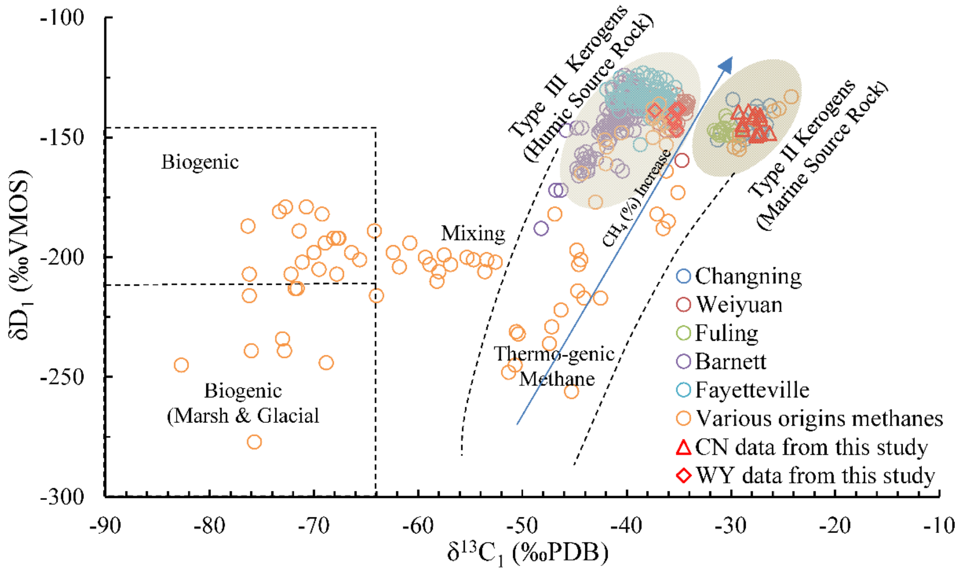

Fig. 7 *Relationship between hydrogen and carbon isotope configurations of methane in various origins facilitating the differentiation of genetic groups. Longmaxi shale gases from the Weiyuan and Changning sectors in Sichuan Basin, China (data sources: Xu et al., 2018; Yang et al., 2017; Feng et al., 2016, 2018; Dai et al., 2016; this study), and Barnett and Fayetteville shale gases (Zumberge et al., 2012). All fall into the "thermogenic methane" area (after Schoell et al., 1980).*

Carbon isotopic composition in this and previous studies (Dai *et al.*, 2014b; Gao *et al.*, 2015; Cao *et al.*, 2016; Feng *et al.*, 2016) all suggest that Longmaxi Formation shale gases in Sichuan Basin underwent a high-thermal-evolution stage. The evolution of shale gases can be divided into three zones according to $\delta^{13}C_2$ versus wetness (Xia *et al.*, 2013; Tilley and Muehlenbachs, 2013): a pre-rollover zone (wetness > 8.0%), rollover zone (0.8% < wetness < 8.0%), and post-rollover zone (wetness < 0.8%) (Zumberge *et al.*, 2012; Feng *et al.*, 2016) [Fig. 8(a)]. Barnett and Fayetteville shale gases primarily belong to the rollover zone, while WY and CN shale gases are mainly distributed in the post-rollover area [Fig. 8(a)], in which $\delta^{13}C_2$ has a negative correlation with wetness. This phenomenon illustrates that WY and CN shale gases are all over-matured (2.00%<Ro<2.20%). Furthermore, with the evolution of shale gases (from low mature state to over-mature state), not only does the content of methane increase but so does the $\delta^{13}C_1$ (Dai *et al*., 2016; Feng *et al*., 2016; Tilley and Muehlenbachs, 2013). As revealed in Fig. 8(b), CN, Fuling, and WY shale gases have heavier methane carbon isotopic composition than Barnett and Fayetteville shale gases. This indicates that shale gases in the WY and CN areas have reached a higher evolution stage.

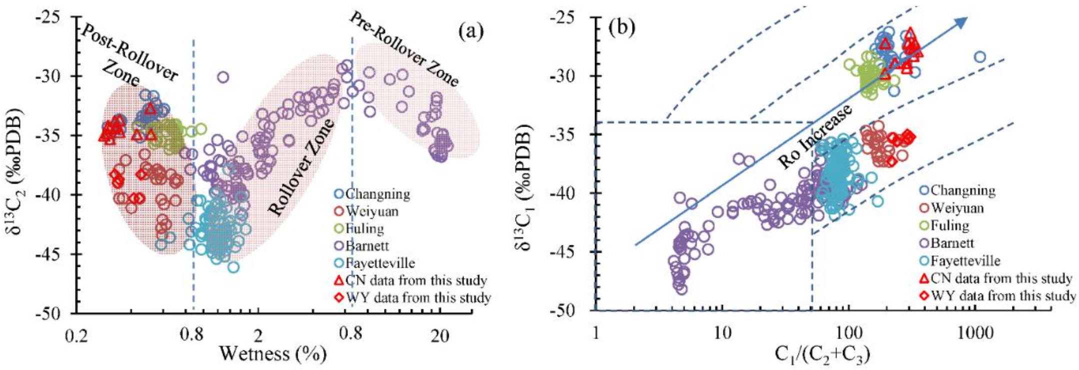

Fig. 8 *(a) Wetness-dependent variation of $\delta^{13}C_2$ in shale gases in Weiyuan and Changning sectors compared with shale gases from Fuling, Barnett, and Fayetteville fields. (b) Modified Bernard diagram showing that $\delta^{13}C_1$ of shale gas increases with increasing maturity (data sources: Xu et al., 2018; Yang et al., 2017; Gao et al.,2016; Feng et al., 2016, 2018; Dai et al., 2016; Zumberge et al., 2012; this study). Wetness (%) = $C_{2+}/(C_1+C_{2+})$.*

A relationship between $\ln(C_1/C_2)$ vs. $\ln(C_2/C_3)$ has been established based on simulation experiments to discriminate kerogen-cracking gas and oil-cracking gas in a sealed system (Liu *et al*., 2018; Yang *et al*., 2017; Li *et al*., 2015). Figure 9 shows that Longmaxi Formation shale gases in the WY and CN areas are all comprised of kerogen-and oil-cracking gases, but mainly the latter. In contrast, most of the Barnett and Fayetteville shale gases are generated from kerogen cracking, even though they are all derived from a mixture of primary and secondary cracking gases. WY shale gases include more oil-cracking gas than CN shale gases, which suggests that WY shale gases are not generated from humic source rock (Type-III kerogen), but more like come from Type I-II organic matter.

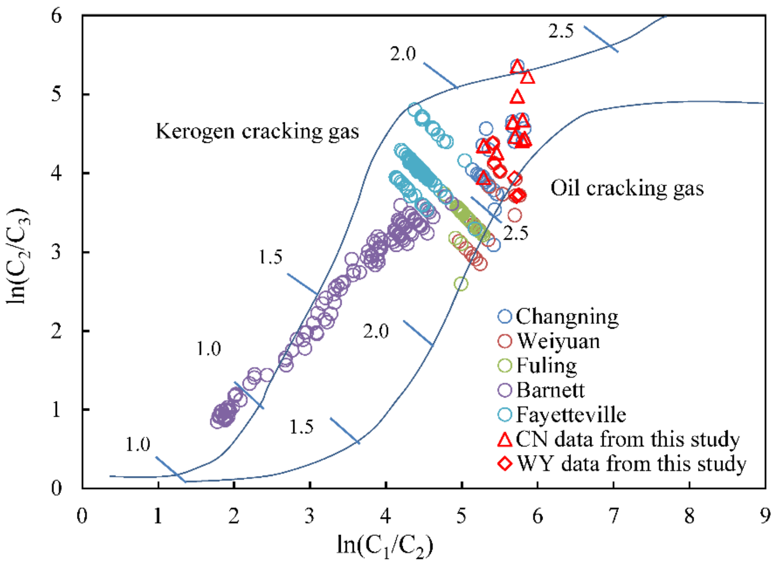

Fig. 9 *Plot of $ln(C_1/C_2)$ vs. $ln(C_2/C_3)$ to discriminate the kerogen- and oil-cracking gases with increasing Ro value (%) (data sources: Xu et al., 2018; Zhang et al., 2018; Yang et al., 2017; Feng et al., 2016, 2018; Dai et al., 2016; Zumberge et al., 2012; this study). These variations suggest that gases from the CN, WY, and Fuling fields were obtained from secondary oil cracking. In comparison, the majority of Barnett shale gases originated via the primary cracking of kerogen, whereas gas samples from Fayetteville, Appalachian Basin, and Barnett Shale were obtained via a combination of primary and secondary cracking gases. (After Liu et al., 2018; Yang et al., 2017; Li et al., 2015.)*

5.2 Origin of carbon dioxide

There is a certain amount of CO_2 (0.03%–1.35%) in Longmaxi formation shale gases. The genesis of CO_2 helps us learn more about shale gas sources. CO_2 sources in shale gases include thermal decomposition of carbonates, microbial degradation of the organic substrates, thermal maturation of kerogen, dissolved atmospheric CO_2, soil gas, and magmatic/mantle degassing (Zhang *et al.*, 2008; Dai *et al.*, 1996, Wycherley *et al.*, 1999; Zumberge *et al.*, 2012). The wide range of $\delta^{13}C_{CO2}$ values suggests that the CO_2 in Longmaxi shale gases has multiple origins (Fig. 10).

The association between concentration and carbon isotopic composition (CO_2 abundance versus $\delta^{13}C_{CO2}$; see Fig. 10) can be used to evaluate the origin of CO_2 (Boreham *et al.*, 2001; Zhang *et al.*, 2008). Gases that have CO_2<10% and −10‰<$\delta^{13}C_{CO2}$<−3‰ are likely mixtures of organic or thermogenic CO_2 affected by microbial degradation (Golding *et al.*, 2013). Longmaxi shale gases have a CO_2 content between 0.03% and 1.35% (Table 1) and carbon isotope ratios in the range from −8.9‰ to −0.8‰ (Table 2). CO_2 in Longmaxi shale gases is enriched in the heavier carbon isotope ^{13}C, and $\delta^{13}C_{CO2}$ values are normally higher than -3‰ (Fig. 10). Abiogenic-derived CO_2, *i.e.*, decarbonized CO_2 (Mattey *et al.*, 1990; Huang *et al.*, 2004) or mantle degassing (Marty and Tolstikhin, 1998) is generally isotopically heavier. The inorganic $\delta^{13}C_{CO2}$ value of thermal cracking of carbonate minerals is near that of the $\delta^{13}C$ value of carbonate rock, approximately 0±3‰ (Dai *et al.*, 1995). Furthermore, Linxiang and Baota formations, which are dominated by limestone below the Longmaxi Formation shale, can be the source of decomposition of carbonate (Chen *et al.*, 2014; Feng *et al.*, 2018). Although CO_2 in WY, CN, Fuling, Barnett, and Fayetteville shale gases is mainly generated from the transformation of organic matter, WY and CN shale gases also contain an endogenic CO_2 that may be associated with Emei mantle plume activity. This can be seen in the plot of $\delta^{13}C_{CO2}$ versus $\delta^{13}C_1$ (Fig. 11). Endogenic CO_2 in WY and CN shale gases are produced at different temperatures. In the WY area, CO_2 is generated by decomposition of carbonate at 200ºC–300ºC, but the temperature for carbonate decomposition is 300 ºC–400 ºC in the CN area (Fig. 11).

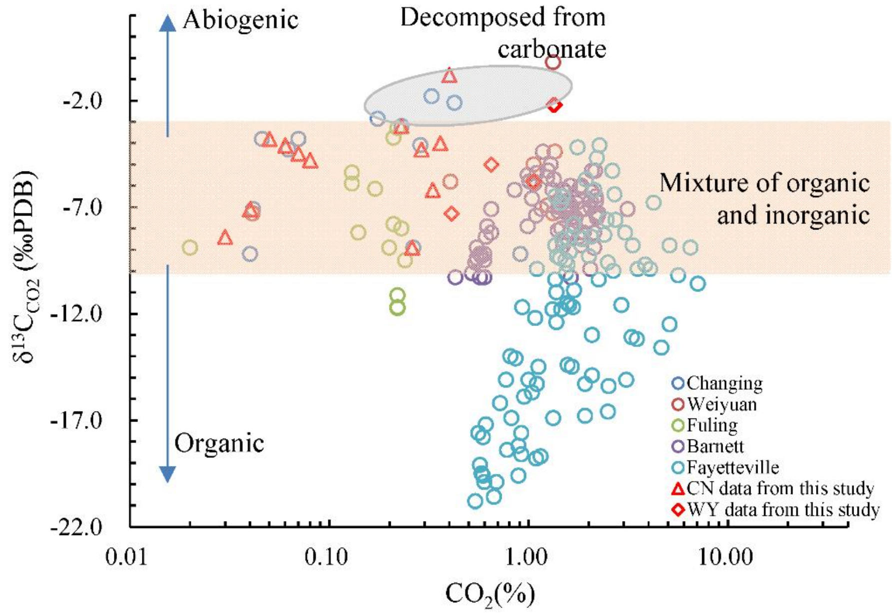

Fig. 10 *Plot of CO_2 content vs $\delta^{13}C_{CO2}$ showing the origin of the CO_2 in shale gases (data sources: Xu et al., 2018; Zhang et al., 2018; Yang et al., 2017; Feng et al., 2016, 2018; Dai et al., 2016; Zumberge et al., 2012; this study). Gases with CO_2 contents lower than 10% exhibited a broad span of $\delta^{13}C$ values. Thermogenic CO_2 sourced from coal or organic matter in shales were variably lowered in ^{13}C, as what is observed in the Fayetteville shale gas, whereas isotopically heavy CO_2 (>−3‰) residual was observed following the decomposition product of carbonate. Gases with CO_2 contents lower than 10% and carbon isotope compositions in the inorganic span within −3% and −10‰ were frequently combinations or thermogenic CO_2 impacted by the decomposition of carbonate.*

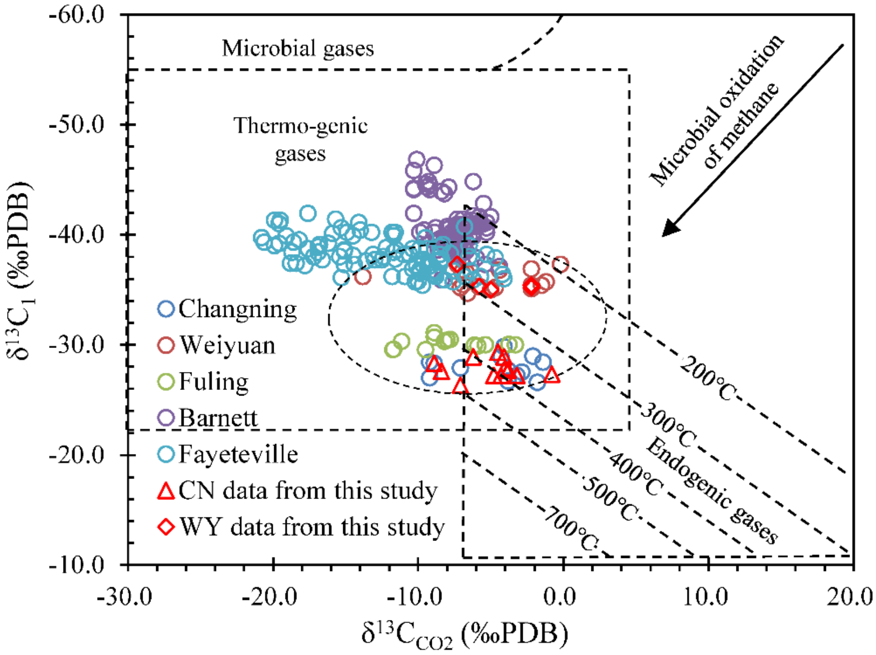

Fig. 11 *Genetic characterization of analyzed shale gases using $\delta^{13}C_1$ vs $\delta^{13}C_{CO2}$ (data sources: Xu et al., 2018; Zhang et al., 2018; Yang et al., 2017; Feng et al., 2016, 2018; Dai et al., 2016; Zumberge et al., 2012; this study) (according to Gutsalo and Plotnikov, 1981; Kotarba et al., 2014). $\delta^{13}C_{CO2}$ values of upper mantle varied from −8% to −5% (average: approximately −7%) (e.g., Pineau et al., 1976; Javoy et al., 1986). Carbon dioxide from Weiyuan and Changning shale reservoirs contain an endogenic component (magmatic-and/or upper-mantle-derived). Weiyuan and Changning lie in the Emeishan basalt province and adjacent regions (Zhu et al., 2010b), which are affected by a thermal anomaly and by diffuse CO_2 degassing.*

Based on $^{3}He/^{4}He$ ratios, which span from 0.001 to 0.019 Ra (Ra is atmospheric value=1.4 × 10^{-6}) (Table 3), there is no CO_2 derived from magmatic/mantle degassing in the Longmaxi Formation shale gases (Cao *et al.*, 2016; Liu *et al.*, 2018). The lower CO_2 contents in WY and CN shale gases may be due to CO_2's elevated aqueous solubility in subsurface formation waters and diagenetic reactivity with subsurface strata (Kotarba *et al.*, 2008, 2014).

5.3 Origin of Nitrogen

Nitrogen is also an important component in shale gases, which tell us the atmosphere and crustal endmembers' infusion. In $N_2/^{40}Ar$ versus $^{36}Ar/^{40}Ar$ space, most Longmaxi shale-gas samples plot between the crustal, radiogenic, and atmospheric elements (Fig. 12). It shows that Ar and N_2 in WY and CN shale gases contain atmospheric Ar and N_2, which is typically observed in crustal fluid studies (Ballentine *et al.*, 1991) and originates from sedimentation water or groundwater that had previously equilibrated with air (Battani *et al.*, 2000). However, the difference in $N_2/^{40}Ar$ and $^{36}Ar/^{40}Ar$ ratios across the Longmaxi Formation shale gases (Fig. 12) is not consistent with simple two-component mixing between atmosphere and crustal endmembers. The variable $^{36}Ar/^{40}Ar$ is caused by the accumulation of ^{40}Ar produced from ^{40}K, but variable $N_2/^{40}Ar$ at an approximately constant $^{36}Ar/^{40}Ar$ imply that the nitrogen cannot be explained by mixing with a dissolved air component.

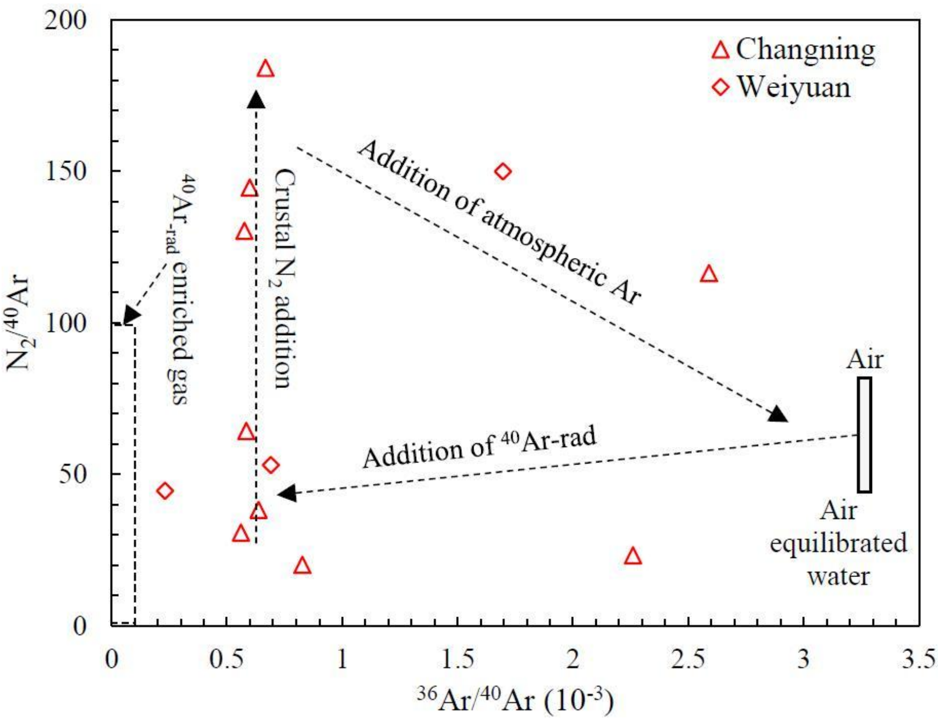

Fig. 12 *Plot of $N_2/^{40}Ar$ vs. $^{36}Ar/^{40}Ar$ displaying a dissolved-air groundwater N_2 contribution that is not in agreement with simple two-component mixing among the atmosphere and crustal endmembers, demonstrating that nitrogen could not be explained by simple mixing dissolved air components. Square labelled "$^{40}Ar_{-rad}$ enriched gas" shows the region in which low $N_2/^{40}Ar$ ratio results from accumulation of ^{40}Ar produced from ^{40}K. Rectangle in lower right-hand corner denotes N_2/Ar ratio for air (84) and for fractionated air dissolved in water (~ 40).*

In CN shale gas, there is an apparent increasing trend of crustal N_2 addition (Fig. 12). This is also demonstrated by Fig. 13, in which all data shows that noble gases in Longmaxi shale gases are crustal in origin with no mantle-derived volatile component. Evidence was found for significant nitrogen storage as NH_4^+ during diagenesis in shales (Krooss et al., 2006) and, furthermore, nitrogen can be produced in great quantities during the thermogenic transformation of organic matter (Krooss et al., 1995). The process of molecular nitrogen production from organic matter was documented by pyrolytic experiments (Gerling et al., 1997). Organic N in present biogenic materials such as marine plants, animals and sediments shows a wide range of $\delta^{15}N$ values from -8 to +23‰ (Sano et al., 1993).

Nitrogen isotopic composition varies in Earth's major reservoirs ($\delta^{15}N$ = 0‰ for atmospheric, Li et al., 2009; −5 ± 3‰ for the mantle, Marty and Zimmermann, 1999, Cartigny et al., 2001 and +2‰<$\delta^{15}N$<+10‰ for crustal rocks, Bebout and Fogel, 1992). Nitrogen isotope data are needed to confirm if there are N_2 generated by thermogenic transformation of organic matter in WY and CN shale gases.

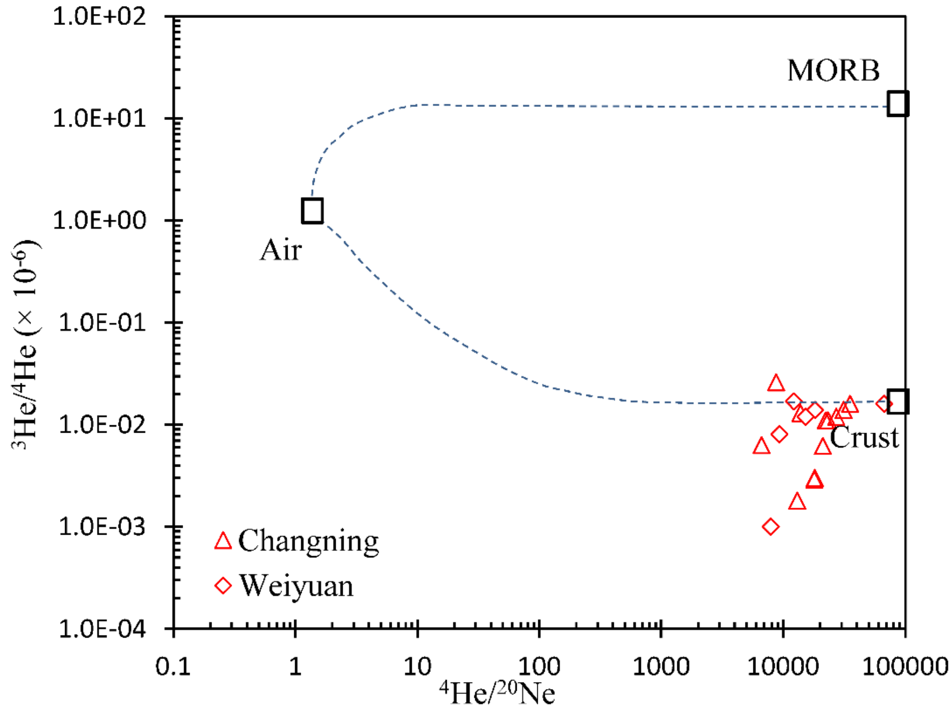

Fig. 13 *Plot of $^3He/^4He$ vs $^4He/^{20}Ne$ showing mixing lines among the atmosphere and the upper mantle and between the atmosphere and the crust. Curved lines joining the air-upper mantle and air-crust were determined utilizing the endmembers: atmosphere ($^3He/^4He$=1.4 × 10^{-6}, $^4He/^{20}Ne$=0.318) (Ozima and Podosek, 2002), continental crust ($^3He/^4He$=0.01 × 10^{-6}, $^4He/^{20}Ne$=100,000) (Ballentine and Burnard, 2002), and upper mantle ($^3He/^4He$=12 × 10^{-6}, $^4He/^{20}Ne$=100,000) (e.g., Graham, 2002).*

5.4 Origin of shale gases from noble gas perspective

Being chemically inert and having distinct isotopic composition in atmosphere, crust, and mantle (Ozima and Podosek, 2002; Hilton *et al*., 2003), noble gases have become one of the ideal natural tracers for studying the origin and evolution of crustal fluids in sedimentary basins(Wen *et al*., 2017; Pinti *et al*., 2013; Procellli *et al*., 2002). They play a unique role in tracing atmospheric, radiogenic, and mantle-derived gases.

The $CH_4/^3He$ vs. R/Ra plot (Fig. 14) shows that all shale gases from Longmaxi Formation in WY and CN areas, Sichuan Basin, lie at the crustal end ($CH_4/^3He$ = 3×10^{13}, R/Ra = 0.01; Jenden et al., 1993), far from the abiotic values of EPR (geothermal fluids from 21°N East Pacific Rise; Welhan and Craig, 1983) and ZO (gas seeps from the Zambales Ophiolite in the Philippines; Abrajano et al., 1988).

Although having a similar distribution of $CH_4/^3He$ vs. R/Ra, conventional natural gases show a slightly higher $CH_4/^3He$ ratio than WY and CN shale gases. Gases from Bohai Bay, Songliao Basin and Hotspring in China have a lower $CH_4/^3He$ ratio and higher R/Ra than Longmaxi shale gases and conventional natural gases, which indicates their different origins.

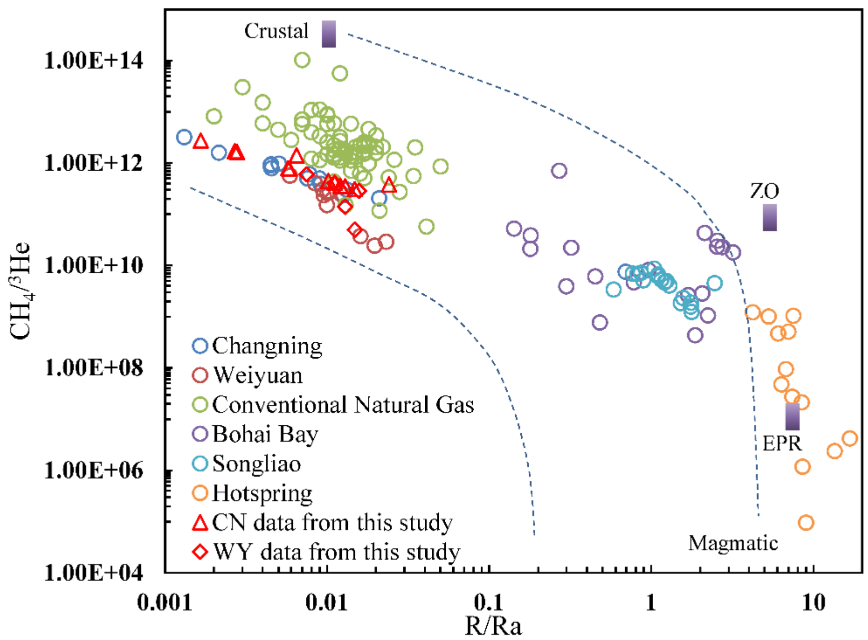

Fig. 14 *$CH_4/^3He$ vs R/Ra plot of shale gases from the Longmaxi Formation of the Weiyuan and Changning sectors in the Sichuan Basin, China (data from this study). Also shown are conventional gases from East Sichuan, Central Sichuan, and Ordos (Dai et al., 2008; Ni et al., 2014) and gases from Bohai Bay (Dai et al., 2008), Hotspring (Sano et al., 1985), and Songliao Basin (Dai et al., 2008), implying the addition of mantle-derived helium. EPR, geothermal fluids from East Pacific Rise (Welhan and Craig, 1983; Niedermann et al., 1997); ZO, gas seeps from Zambales Ophiolite, which were collected from the Philippines (Abrajano et al., 1988); crustal values are from Jenden et al.(1993).*

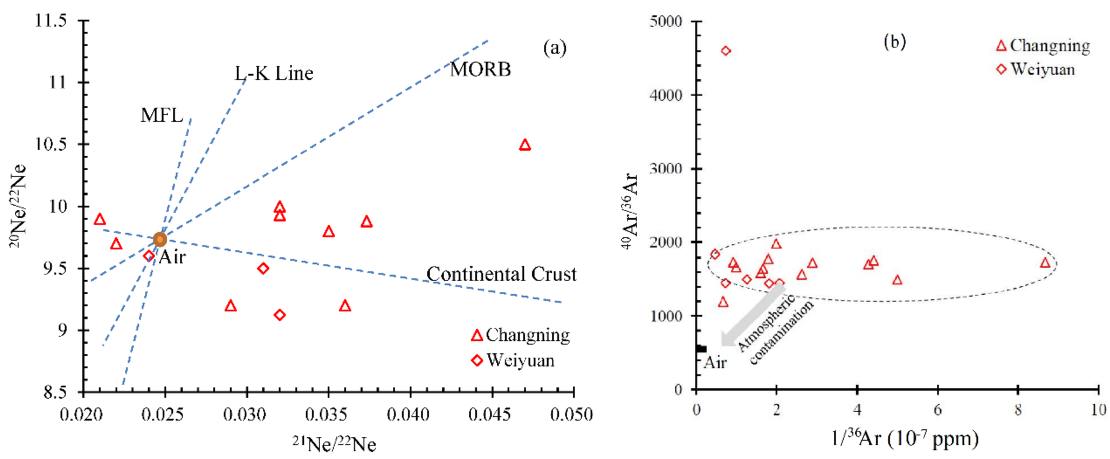

***Fig. 15** Plots of (a) neon isotopes and (b) $^{40}Ar/^{36}Ar$ vs $1/^{36}Ar$. Mass fractionation line (MFL), Loihi–Kilauea (L-K) line (air-plume mixing; Honda et al., 1991), MORB line (air-MORB mixing; Sarda et al., 1988), and air-crust mixing line (Kennedy et al., 1990) are shown for reference.*

Within the Ne three-isotope plot [Fig. 15(a)], although information associated with atmospheric neon indicates that Ne is atmospherically derived in Longmaxi shale gases, the crust-derived (radiogenic origin) compositions apparently account for a large proportion. When $^{40}Ar/^{36}Ar$ data are plotted versus the reciprocal of the ^{36}Ar concentrations [Fig. 15(b)], the $^{40}Ar/^{36}Ar$ ratios also define a radiogenic endmember ($1194.3<^{40}Ar/^{36}Ar<4604.5$), which is common to all the WY and CN shale gases. Radiogenic ^{40}Ar is the product of radiogenic decay of K either from the sedimentary rocks or from the basement. Moreover, the $^{40}Ar/^{36}Ar$ ratios are consistent with the age of Longmaxi strata calculated by the age accumulative effect of Ar isotope (Zheng *et al*., 2005; Liu and Xu, 1993). WY shale gases have lower $^{40}Ar/^{36}Ar$ and $1/^{36}Ar$ ratios, which is closer to an air-endmember, whereas, CN shale gases have high $^{40}Ar/^{36}Ar$ and $1/^{36}Ar$ ratios. Even if there is more radiogenic ^{40}Ar derived from radioactive decay of K in the CN area (Gu *et al*., 2012), the $1/^{36}Ar$ ratios cannot possibly be larger than those in the WY area. However, atmospherically derived Ar is more easily degassed from sedimentation water or groundwater in WY shale reservoirs, because of low pressure in shale strata (Cao *et al*., 2018). Therefore, in WY shale gases, atmospherically derived ^{36}Ar content is higher than that in CN shale gases, which made $1/^{36}Ar$ ratios low in the WY area. This may also be the reason for more N_2 in the WY shale gas than that in the CN shale gas (Fig. 3 and Table 1).

6. Conclusions

The present study investigated the stable isotopic composition of noble gases (He, Ne, Ar, Kr, and Xe) and molecular compositions of shale gases collected in the Lower Silurian Longmaxi Formation of Southern Sichuan Basin in Weiyuan (WY) and Changning (CN), China, specifically their stable carbon isotopic compositions of the hydrocarbons (CH_4, C_2H_6, and C_3H_8) and CO_2 and the stable hydrogen isotopic compositions of methane and ethane. The WY and CN shale gases are comprised mainly of CH_4 (93.41%–99.0%), while non-hydrocarbon gases primarily include N_2 (0.22%–2.81%) and CO_2 (0.03%–1.35%). H_2S was not detected. The $\delta^{13}C_1$ and $\delta^{13}C_2$ values are different in the WY and CN areas. Carbon- and hydrogen-isotope compositions all display a reversal pattern. The $\delta^{13}C_{CO2}$ values have a wide range, from −8.9‰ to −0.8‰. Kr and Xe exhibit air-like isotope ratios, $^{3}He/^{4}He$ ratios span from 0.001 to 0.019 Ra, and $^{40}Ar/^{36}Ar$ ratios have higher values than they do in air.

The source and thermal evolution history of shale gas in the Silurian Longmaxi Formation of the Sichuan Basin were discussed by suing shale gas geochemical data. WY and CN shale gases come from Type I-II and II organic matter, WY shale gases content more oil-cracking gases. The complete reversal distribution patterns of carbon isotopic composition imply Longmaxi Formation shale gas in the WY and CN regions underwent a high/over-thermal-evolution stage. Thermo-genic CO_2 and N_2 indicate Linxiang and Baota formations may provide gases into Longmaxi shale gas, and Emeishan mantle plume provides the additional source of heat. However, the low helium isotopic composition ($^3He/^4He$: 0.001Ra to 0.019Ra) indicates that no mantle-derived components were injected into the Longmaxi Formation shale gas, which indicates that the Emeishan mantle plume only provides thermal radiation energy and there is no channel between the mantle plume and the Longmaxi Formation shale.

Shale gases in Changning (CN)-Weiyuan (WY) National Shale Gas Demonstration Zone has extremely high CH_4 content (up to 99.01%) and quite heavy $\delta^{13}C_1$ (up to −26.3‰). Carbon isotopic composition of Longmaxi Formation shale gas in Changning (CN)-Weiyuan (WY) National Shale Gas Demonstration Zone exhibit partial reversal ($\delta^{13}C_2<\delta^{13}C_1$ and $\delta^{13}C_2< \delta^{13}C_3$) and complete reversal distribution patterns ($\delta^{13}C_1>\delta^{13}C_2>\delta^{13}C_3$). It turns out that, in shale gas reservoirs (sealed systems), methane content and carbon isotope ratio increase with the degree of thermal evolution. The increase of maturity will also cause carbon isotope reversal. Therefore, low humidity, heavy $\delta^{13}C_1$, and carbon isotope reversal may indicate the overpressure in shale gas reservoir and high yield of shale gas

Acknowledgments

This evaluation was financially assisted by the National Science Foundation of China (41502143) and the Key Laboratory Project of Gansu Province (1309RTSA041). The authors would like to thank Yongli Wang, Hui Yang, Zhongfu Chen, and Wenchang Li for their help in gathering specimens and experimental evaluations.

References

Abrajano T.A., Sturchio N.C., Bohlke J.K., Lyon G.L., Poreda R.J., Stevens C.M., 1988. Methane-hydrogen gas seeps, Zambales Ophiolite, Philippines: Deep or shallow origin? Chem. Geol. 71(1-3), 211-222.

Allegre C.J., Staudacher T., 1987. Sarda P. Rare gas systematics: formation of the atmosphere, evolution and structure of the Earth's mantle. Earth Planet. Sci. Lett. 81(2), 127-150.

Ballentine C.J., Burnard P.G., 2002. Production, release and transport of noble gases in the continental crust. Noble Gases in Geochemistry and Cosmochemistry, Vol. 47 (ed. Porcelli D. R., Ballentine C. J., and Weiler R.), 481-538.

Ballentine C.J., Marty B., Sherwood L.B., 2005. Cassidy M. Neon isotopes constrain convection and volatile origin in the Earth's mantle. Nature. 433(7021), 33-38.

Ballentine C.J., O'Nions R.K., Oxburgh E.R., Horvath F., Deak J., 1991. Rare gas constraints on hydrocarbon accumulation, crustal degassing and groundwater flow in the Pannonian Basin. Earth Planet. Sci. Lett. 105(1-3), 229-246.

Battani A., Sarda P., Prinzhofer A., 2000. Basin-scale natural gas source, migration and trapping traced by noble gases and, elements: the Pakistan Indus basin. Earth Planet. Sci. Lett. 181(1), 229-249.

Bebout G.E., Fogel M.L., 1992. Nitrogen-isotope compositions of metasedimentary rocks in the Catalina Schist, California: implications for metamorphic devolatilization history. Geochim. Cosmochim. Acta. 56, 2839-2849.

Behar, F., Vandenbroucke, M., Teermann, S.C., Hatcher, P.G., Leblond, C., Lerat, O., 1995. Experimental simulation of gas generation from coals and a marine kerogen. Chem. Geol. 126, 247-260.

Boreham C.J., Golding S.D., Glikson M., 2001. Reply to Comment of Smith and Pallasser on “Factors controlling the origin of gas in Australian Bowen Basin coals”. Org. Geochem. 32(1), 207-210.

Burnard P., Graham D., Turner G., 1997. Vesicle-specific noble gas analyses of “popping rock”: implications for primordial noble gases in earth. Science, 276, 568-571.

Cao C.H., Lv Z.G., Li L.W., Du Li., 2016. Geochemical characteristics and implications of shale gas from the Longmaxi Formation, Sichuan Basin, China. J. Nat. Gas Geosci. 1, 131-138.

Cao C.H., Zhang M.J., Tang Q.Y., Yang Y., Lv Z.G., Zhang T.W., Chen C., Yang H., Li L.W., 2018. Noble gas isotopic variations and geological implication of Longmaxi shale gas in Sichuan Basin, China. Mar. Pet. Geol. 89(1), 38-46.

Cartigny P., Jendrzejewski N., Pineau F., Petit E., Javoy M., 2001. Volatile (C, N, Ar) variability in MORB and the respective roles of mantle source heterogeneity and degassing: the case of the Southwest Indian Ridge. Earth Planet. Sci. Lett. 194, 241-257.

Chen S.B., Zhu Y.M., Qin Y., Wang H.Y., Liu H.L., Fang J.H., 2014. Reservoir evaluation of the Lower Silurian Longmaxi Formation shale gas in the southern Sichuan Basin of China. Mar. Pet. Geol. 2014, 57, 619-630.

Dai J.X., Chen J.F., Zhong N.N., 2003. The giant gas fields and their source in China. Science Press. Beijing.

Dai J.X., Ni Y.Y., Huang S.P., Liao F.R., Yu C., Gong D.Y., Wu W., 2014a. Significant function of coal-derived gas study for natural gas industry development in China. Natural Gas Geoscience, 24(1), 1-22.

Dai J.X., Song Y., Dai C.S., Wang D.R., 1996. Geochemistry and accumulation of carbon dioxide gases in China. AAPG Bull. 80, 1615-1626.

Dai J.X., Yan S., Dai C.S., et al., 1995. Conditions governing the formation of abiogenic gas and gas pools in Eastern China. Science Press. Beijing, 17-20.

Dai J.X., Zou C.N., Dong D.Z., Ni Y.Y., Wu W., Gong D.Y., Wang Y.M., Huang S.P., Huang J.L., Fang C.C., Liu D., 2016. Geochemical characteristics of marine and terrestrial shale gas in China. Mar. Pet. Geol. 76, 444-463.

Dai J.X., Zou C.N., Liao S.M., Dong D.Z., Ni Y.Y., Huang W.H., Gong D.Y., Huang S.P., Hu G.Y., 2014b. Geochemistry of the extremely high thermal maturity longmaxi shale gas, southern Sichuan basin. Org. Geochem. 74, 3-12.

Dai J.X., Zou C.N., Zhang S.C., Li J., Ni Y.Y., Hu G.Y., Luo X., Tao S.Z., Zhu G.Y., Mi J.K., Li Z.S., Hu A.P., Yang C., Zhou Q.H., Shuai Y.H., Zhang Y., Ma C.H., 2008. Discrimination of abiogenic and biogenic alkane gases. Sci. China, Ser. D Earth Sci. 51, 1737-1749.

Darrah T.H., Vengosh A., Jackson R.B., Warner N.R., Poreda R.J., 2014. Noble gases identify the mechanisms of fugitive gas contamination in drinking-water wells overlying the Marcellus and Barnett Shales. PNAS. 111(39), 14076-14081.

Dong D.Z., Zou C.N., Dai J.X., Huang S.P., Zheng J.W., Gong J.M., Wang Y.M., Li X.J., Guan Q.Z., Zhang C.C., Huang J.L., Wang S.F., Liu D.X., Qiu Z., 2016. Suggestions on the development strategy of shale gas in China. J. Nat. Gas Geosci. 1(6), 413-423.

Feng Z.Q., Dong D.Z., Tian J.Q., Qiu Z., Wu W., Zhang C., 2018. Geochemical characteristics of Longmaxi Formation shale gas in the Weiyuan area, Sichuan Basin, China. J. Petrol. Sci. Eng. 167, 538-548.

Feng Z.Q., Liu D., Huang S.P., Wu W., Dong D.Z., Peng W.L., Han E.X., 2016. Carbon isotopic composition of shale gas in the Silurian Longmaxi Formation of the Changning area, Sichuan Basin. Pet. Explor. Dev. 43(5), 769-777.

Gao B., 2015. Geochemical characteristics of shale gas from Lower Silurian Longmaxi Formation in the Sichuan Basin and its geological significance. J. Nat. Gas Geosci. 26(6), 1173-1182.

Gao B., 2016. Geochemical characteristics and geological significance of shale gas from the Lower Silurian Longmaxi Formation in Sichuan Basin, China. J. Nat. Gas Geosci. 1(2), 119-129.

Gao L., Schimmelmann A., Tang Y., Mastalerz M., 2014. Isotope rollover in shale gas observed in laboratory pyrolysis experiments: insight to the role of water in thermogenesis of mature gas. Org. Geochem. 68, 95-106.

Gerling, P., Idiz, E., Everlien, G., Sohns, E., 1997. New aspects on the origin of nitrogen in natural gas in Northern Germany. Geol. Jahrb. 103, 65-84.

Golding S.D., Boreham C.J., Esterle, J.S., 2013. Stable isotope geochemistry of coal bed and shale gas and related production waters: A review. Int. J. Coal Geol. 120, 24-40.

Gonzalez-Penagos F., Rouchon V., Guichet X., Moretti I., 2016. The distribution of thermogenic, bacterial and inorganic fluid sources in the petroleum systems of the Llanos Basin (Colombia)-Insights from the noble gases and carbon stable isotopes. Mar. Pet. Geol. 71, 391-403.

Graham D.W., 2002. Noble Gas Isotope Geochemistry of Mid-Ocean Ridge and Ocean Island Basalts: Characterization of Mantle Source Reservoirs. Geochem. Soc. Mineral. Soc. 47(1), 247-317.

Gu M., Xian X.F., Du Y.G., Lu Y.Y., 2012. The inorganic composition, structure and adsorption properties of the shale cores from the Weiyuan gas reservoirs, Sichuan Basin. Nat. Gas. Ind., 32(6), 99-102(in Chinese).

Guo T.L., 2016. Key geological issues and main controls on accumulation and enrichment of Chinese shale gas. Pet. Explor. Dev. 43(3), 349-359.

Gutsalo L.K., Plotnikov A.M., 1981. Carbon isotopic composition in the CH_4-CO_2 system as a criterion for the origin of methane and carbon dioxide in Earth natural gases (In Rusian, English summary). Doklady Akademyi Nauk SSSR, 259, 470-473.

Hao F., Guo T.L., Zhu Y.M., Cai X.Y., Zou H.Y., Li Pi.P., 2008. Evidence for multiple stages of oil cracking and thermochemical sulfate reduction in the Puguang gas field, Sichuan Basin, China. AAPG Bull. 92(5), 611-637.

Hao F., Zou H., 2013. Cause of shale gas geochemical anomalies and mechanisms for gas enrichment and depletion in high-maturity shales. Mar. Pet. Geol. 44, 1-12.

Hilton D.R., Porcelli D., 2003. Noble Gases as Mantle Tracers. Treatise on Geochemistry. Vol. 2.06 (ed. Holland H.D., Turekian K.K.), 277-318.

Honda M., McDougall I., Patterson D.B., Doulgeris A., Clague D.A., 1991. Possible solar noble-gas component in Hawaiian basalts. Nature. 349, 149-151.

Huang B. J., Xiao X. M., Zhu W. L., 2004. Geochemistry, origin, and accumulation of CO_2 in natural gases of the Yinggehai Basin, offshore South China Sea. AAPG Bull. 88, 1277-1293.

Huang J.L., Ju C.N., Li J.Z., Dong D.Z., Wang S.J., Wang S.Q., Wang Y.M., Li D.H., 2012. Shale gas accumulation conditions and favorable zones of Silurian Longmaxi Formation in south Sichuan Basin, China. Journal of China Coal Society. 37(5), 782-787 (in Chinese).

Huang J.Z., Chen S.J., Song J.R., Wang L.S., Gou X.M., Wang T.D., Dai H.M., 1997. Hydrocarbon source systems and formation of gas fields in Sichuan Basin. Sci. China, Ser. D Earth Sci. 40, 32-42.

Javoy M., Pineau F., Delorme H., 1986. Carbon and nitrogen isotopes in the mantle. Chem. Geol. 57(1-2), 41-62.

Jenden P.D., Hilton D.R., Kaplan I.R., Craig H., 1993. Abiogenic hydrocarbons and mantle helium in oil and gas fields. (ed. Howell D.G.), The Future of Energy Gases, Professional Paper 1570, United States Geological Survey, 31-57.

Jiang H.Y., Song X.M., An X.X., Qi R.L., Qiao W.J., Dong L.J., 2008. Overview of shale gas resources and exploration and development technologies in the world. Natural Gas Technology and Economy, 2(6), 26-30 (in Chinese).

Kennedy B.M., Hiyagon H., Reynolds J.H., 1990. Crustal neon: a striking uniformity. Earth Planet. Sci. Lett., 98, 277-286.

Kotarba M.J, Nagao K., 2008. Composition and origin of natural gases accumulated in the Polish and Ukrainian parts of the Carpathian region: Gaseous hydrocarbons, noble gases, carbon dioxide and nitrogen. Chem. Geol. 255(3), 426-438.

Kotarba M.J., Więcław D., Dziadzio P., Kowalski A., Kosakowski P., Bilkiewicz E., 2014. Organic geochemical study of source rocks and natural gas and their genetic correlation in the eastern part of the Polish Outer Carpathians and

Palaeozoic-Mesozoic basement. Mar. Pet. Geol. 56(4), 97-122.
Krooss B.M., Jurisch A., Plessen B., 2006. Investigation of the fate of nitrogen in Palaeozoic shales of the Central European Basin. J. Geochem. Explor. 89(1-3), 191-194.
Krooss B.M., Littke R., Müller B., Frielingsdorf J., Schwochau K., Idiz E.F., 1995. Generation of nitrogen and methane from sedimentary organic matter: Implications on the dynamics of natural gas accumulations. Chem. Geol. 126(3-4), 291-318.
Lee J.Y., Marti K., Severinghaus J.P., Kawamura K., Yoo H.S., Lee J.B., Kim J.S., 2006. A redetermination of the isotopic abundances of atmospheric Ar. Geochim. Cosmochim. Acta. 70(17), 4507-4512.
Li J., Xie Z.Y., Wei G., Li Z., Wang W., 2015. Geochemical characteristics and exploration potential of natural gas in Anyue gas field, the largest uncompartmentalized carbonate gas field in China. In: The 15th National Meeting on Organic Geochemistry in China (Qingdao, Shandong, China).
Li L., Cartigny P., Ader M., 2009. Kinetic nitrogen isotope fractionation associated with thermal decomposition of NH_3: Experimental results and potential applications to trace the origin of N_2, in natural gas and hydrothermal systems. Geochim. Cosmochim. Acta. 73(20), 6282-6297.
Li Z.P., Wang X.B., Li L.W., Zhang M.J., Tao M.X., Xing L.T., Cao C.H., Xia Y.Q., 2014. Development of new method of $\delta^{13}C$ measurement for trace hydrocarbons in natural gas using solid phase micro-extraction coupled to gas chromatography isotope ratio mass spectrometry. J. Chromatogr. A. 1372, 228-235.
Liang D.G., Guo T.L., Bian L.Z., Chen J.P., Zhao J.,2009. New advances in the study of marine hydrocarbon accumulation in South China (one). Marine Origin Petroleum Geology. 13(2), 1-16 (in Chinese).
Liang J.T., Huang W.H., Wang H.L., Blum M.J., Chen J., Wei X.L., Yang G.Q., 2020. Organic geochemical and petrophysical characteristics of transitional coal-measure shale gas reservoirs and their relationships with sedimentary environments: A case study from the Carboniferous-Permian Qinshui Basin, China. J. Petrol. Sci. Eng. 184, In press.
Liu C.J., Liu P., McGovern G.P., Horita J., 2019. Molecular and intramolecular isotope geochemistry of natural gases from the Woodford Shale, Arkoma Basin, Oklahoma. Geochim. Cosmochim. Acta. 255(15), 188-204.
Liu Q.Y., Jin Z.J., Li H.L, Wu X.Q., Tao X.W., Zhu D.Y., Meng Q.Q., 2018. Geochemistry characteristics and genetic types of natural gas in central part of the Tarim Basin, NW China. Mar. Pet. Geol. 89(1), 91-105.
Liu S.G., Deng B., Zhong Y.S., Ran B., Yong Z., Sun W., Yang D.Z., Jiang L., Ye Y., 2016. Unique geological features of burial and superimposition of the Lower Paleozoic shale gas across the Sichuan Basin and its periphery. Earth Sci. Front. 23(1), 11-28 (in Chinese).
Liu W.H., Xu Y.C., 1993. Significance of helium and argon isotopic composition in

natural gas. Chin. Sci. Bull. 2(9), 818-821 (in Chinese).

Marty B., Tolstikhin I. N., 1998. CO_2 fluxes from mid-ocean ridges, arcs and plumes. Chem. Geol. 145, 233-248.

Marty B., Zimmermann L., 1999. Volatiles (He, N, C, Ar) in mid-ocean ridge basalts: assessment of shallow-level fractionation and characterization of source composition. Geochim. Cosmochim. Acta. 63, 3619-3633.

Mattey D. P., Taylor W. R., Green D. H., Pillinger C. T., 1990. Carbon isotopic fractionation between CO_2 vapor, silicate and carbonate melts - An experimental study to 30 kbar. Contrib. Mineral. Petrol. 104, 492-505.

Moreira M. 2013. Noble gas constraints on the origin and evolution of Earth's volatiles. Geochemical Perspectives. 2(2), 229-403.

Moreira M., Kunz J., Allegre C., 1998. Rare gas systematics in popping rock: isotopic and elemental compositions in the upper mantle. Cambridge University Press. 279(5354), 1178-1181.

Ni Y.Y., Dai J.X., Tao S.Z., Wu X.Q., Liao F.R., Wu W., Zhang D.J., 2014. Helium signatures of gases from the Sichuan Basin, China. Org. Geochem. 74, 33-43.

Niedermann S., Bach W., Erzinger J., 1997. Noble gas evidence for a lower mantle component in MORBs from the southern East Pacific Rise: decoupling of helium and neon isotope systematics. Geochim. Cosmochim. Acta. 61(13), 2697-2715.

Ozima M., Podosek F.A., 2002. Noble Gas Geochemistry, second ed. Cambridge University Press, Cambridge.

Pineau F., Javoy M., Bottinga Y., 1976. $^{13}C/^{12}C$ ratios of rocks and inclusions in popping rocks of mid-Atlantic ridge and their bearing on problem of isotopic composition of deep-seated carbon. Earth Planet. Sci. Lett. 29, 413-421.

Pinti D.L., Castro C.M., Shouakar-Stash O., Tremblay A., Garduño V.H., Hall C.M., Hélie J.F., Ghaleb B., 2013. Evolution of the geothermal fluids at Los Azufres, Mexico, as traced by noble gas isotopes, $\delta^{18}O$, δD, $\delta^{13}C$ and $^{87}Sr/^{86}Sr$. J. Volcanol. Geotherm. Res. 249(0), 1-11.

Porcelli D., Ballentine C.J., 2002. Models for the distribution of terrestrial noble gases and evolution of the atmosphere. (ed. Porcelli D., Ballentine C.J., Wieler R.), Noble Gases in Geochemistry and Cosmochemistry, Rev Mineral Geochem, 47, 412-480

Rahayudin Y., Kashiwaya K., Tada Y., Iskandar I., Koike K., Atmaja R.W., Herdianita N.R., 2020. On the origin and evolution of geothermal fluids in the Patuha Geothermal Field, Indonesia based on geochemical and stable isotope data. Appl. Geochem. 114, In press.

Rodriguez N.D., Philp R.P., 2010. Geochemical characterization of gases from the Mississippian Barnett shale, Fort Worth Basin, Texas. AAPG Bull. 94, 1641-1656.

Sano Y., Nakamura Y., Wakita H., 1985. Areal distribution of $^{3}He/^{4}He$ ratios in the Tohoku district, Northeastern Japan, Chem. Geol.: Isotope Geoscience section, 52(1), 1-8.

Sano Y., Urabe A., Wakita H., 1993. Origin of hydrogen-nitrogen gas seeps, Oman. Appl. Geochem. 8(1), 1-8.

Sarda P., Staudacher T., Allegre C.J., 1988. Neon isotopes in submarine basalts. Earth Planet. Sci. Lett. 91(1), 73-88.

Schlegel M.E., Zhou Z., Mcintosh J.C., Ballentine C.J., Person M., 2011. Constraining the timing of microbial methane generation in an organic-rich shale using noble gases, Illinois Basin, USA. Chem. Geol. 287(1), 27-40.

Schoell M., 1980. The hydrogen and carbon isotopic composition of methane from natural gases of various origins. Geochim. Cosmochim. Acta. 44, 649-661.

Song D.J., Tuo J.C., Wu C.J., Zhang M.F., Su L., 2020. Comparison of pore evolution for a Mesoproterozoic marine shale and a Triassic terrestrial mudstone during artificial maturation experiments. J. Nat. Gas Sci. Eng. 75, In press.

Tian H., Wang Z.M., Xiao Z.Y., Li X.Q., Xiao X.M., 2006. Oil cracking to gases: Kinetic modeling and geological significance. Chin. Sci. Bull. 51(22), 2763-2770.

Tian H., Xiao X.M., Li X.Q., Xiao Z.Y., 2007. Comparison of gas generation and carbon isotope fractionation of methane from marine kerogen-and crude oil-cracking gases. Geochimica. 36, 71-77 (in Chinese).

Tilley B., Muehlenbachs K., 2013. Isotope reversals and universal stages and trends of gas maturation in sealed, self-contained petroleum systems. Chem. Geol. 339, 194-204.

Tuo J.C., Wu C.J., Zhang M.F., 2016. Organic matter properties and shale gas potential of Paleozoic shales in Sichuan Basin, China. J. Nat. Gas Sci. Eng. 28, 434-446.

Wang C.S., Scott R.W., Wan X.Q., Graham S.A., Huang Y.J., Wang P.J., Wu H.C., Dean W., Zhang L.M., 2013. Late Cretaceous climate changes recorded in Eastern Asian lacustrine deposits and North American Epieric sea strata. Earth Sci. Rev. 126, 275-299.

Wang X.F., Li X.F., Wang X.Z., Shi B.G., Luo X.R., Zhang L.X., Lei Y.H., Jiang C.F., Meng Q., 2015. Carbon isotopic fractionation by desorption of shale gases. Mar. Pet. Geol. 60, 79-86.

Wang Y.P., Hilton D.R., Zhou Z., Zheng G.D., 2017. Progress in the Application of Gas Geochemistry to Geothermal, Tectonic and Magmatic Studies. Chem. Geol. 469(10), 1-3.

Warner N.R., Kresse T.M., Hays P.D., Down A., Karr J.D., Jackson R.B., Vengosh A., 2013. Geochemical and isotopic variations in shallow groundwater in areas of the Fayetteville Shale development, north-central Arkansas. Appl. Geochem. 35, 207-220.

Wei G.Q., Chen G.S., Du S.M., Zhang L., Yang W., 2008. Petroleum systems of the oldest gas field in China: neoproterozoic gas pools in the Weiyuan gas field, Sichuan Basin. Mar. Pet. Geol. 25, 371-386.

Welhan J.A., Craig H. 1983. Methane, Hydrogen and Helium in Hydrothermal

Fluids at 21°N on the East Pacific Rise. (ed. Rona P.A., Boström K., Laubier L., Smith K.L.), Hydrothermal Processes at Seafloor Spreading Centers. NATO Conference Series (IV Marine Sciences), Vol 12. Springer, Boston, MA.

Wen T., Castro M.C., Nicot Jean-Philippe, Hall C.M., Pinti D.L., Mickler P., Darvari R., Larson T., 2017. Characterizing the Noble Gas Isotopic Composition of the Barnett Shale and Strawn Group and Constraining the Source of Stray Gas in the Trinity Aquifer, North-Central Texas. Environ. Sci. Technol. 51(11), 6533-6541.

Wycherley H., Fleet A., Shaw H., 1999. Some observations on the origins of large volumes of carbon dioxide accumulations in sedimentary basins. Mar. Pet. Geol. 16(6), 489-494.

Xia X.Y., Chen J.M., Braun R., Tang Y.C., 2013. Isotopic reversals with respect to maturity trends due to mixing of primary and secondary products in source rocks. Chem. Geol. 339, 205-212.

Xiao X.M., Tian H., Liu D.H., Liu Z.F., 2012. Evaluation of Deep Burial Source Rocks and Their Natural Gas Potentials in Sichuan Basin. Annual Report of State Major Research Program of China (Project No. 2011ZX05008-002-40), Internal Report, Guangzhou Institute of Geochemistry of Chinese Academy of Sciences. 1-68 (in Chinese with English abstract).

Xu H., Zhou W., Cao Q., Xiao C., Zhou Q.M., Zhang H.T., Zhang Y.Y., 2018. Differential fluid migration behavior and tectonic movement in Lower Silurian and Lower Cambrian shale gas systems in China using isotope geochemistry. Mar. Pet. Geol. 89(1), 47-57.

Yang F., Xu S., Hao F., Hu B.Y., Zhang B.Q., Shu Z.G., Long S.Y., 2019. Petrophysical characteristics of shales with different lithofacies in Jiaoshiba area, Sichuan Basin, China: Implications for shale gas accumulation mechanism. Mar. Pet. Geol. 109, 394-407.

Yang R., He S., Hu Q.H., Hu D.F., Yi J.Z., 2017. Geochemical characteristics and origin of natural gas from Wufeng-Longmaxi shales of the Fuling gas field, Sichuan Basin (China). Int. J. Coal Geol. 171, 1-11.

Ye X.R., Tao M. X., 2007. Helium and neon isotopic compositions in the ophiolites from the Yarlung Zangbo River, Southwestern China: The information from deep mantle. Sci. China, Ser. D Earth Sci. 50(6), 801-812.

Zhang M.J., Tang Q.Y., Cao C.H., Lv Z.G., Zhang T.W., Zhang D.K., Li Z.P., Du L., 2018a. Molecular and carbon isotopic compositional variation in 3.5 years shale gas production from Longmaxi Formation in Sichuan Basin, China. Mar. Pet. Geol. 89(1), 27-37.

Zhang M.J., Tang Q.Y., Hu P.Q., Ye X.R., Cong Y.N., 2013. Noble gas isotopic constraints on the origin and evolution of the Jinchuan Ni-Cu-(PGE) sulfide ore-bearing ultramafic intrusion, West. China. Chem. Geol. 339, 301-312.

Zhang S.C., He K., Hu G.Y., Mi J.K., Ma Q.S., Liu K.Y., Tang Y.C., 2018b. Unique chemical and isotopic characteristics and origins of natural gases in the Paleozoic marine formations in the Sichuan Basin, SW China: Isotope fractionation of deep and high mature carbonate reservoir gases. Mar. Pet. Geol. 89(Part 1), 68-82.

Zhang T.W., Zhang M.J., Bai B.J., Wang X.B., Li L.W., 2008. Origin and accumulation of carbon dioxide in the Huanghua depression, Bohai Bay Basin, China. AAPG Bull. 92(3), 341-358.

Zhao W.Z., Yang X.P., Steve K., Zhang B.M., 2006. Reservoir potential of Silurian carbonate mud mounds in the southern Sichuan Basin, central China. Acta Geol. Sin. 80(5), 684-692.

Zheng J.J., Hu H.F., Liu W.H., Zhang D.W., Wang X.F., Sun G.Q., 2005. Discussion about the relationship between helium and argon in research of gas and source rock correlation of natural gas. J. Nat. Gas Geosci. 16(4), 499-502 (in Chinese).

Zhou Q., Xiao X.M., Tian H., Pan L., 2014. Modeling free gas content of the Lower Paleozoic shales in the Weiyuan area of the Sichuan Basin, China, Mar. Pet. Geol. 56, 87-96.

Zhou X.C., Liu L., Chen Z., Cui Y.J., Du J.G., 2019. Gas geochemistry of the hot spring in the Litang fault zone, Southeast Tibetan Plateau. Appl. Geochem. 79, 17-26.

Zhou Z., Ballentine C.J., Kipfer R., Schoell M., Thibodeaux S., 2005. Noble gas tracing of groundwater/coalbed methane interaction in the San Juan Basin, USA. Geochim. Cosmochim. Acta. 69(23), 5413-5428.

Zhu C.Q., Xu M., Yuan Y.S., Zhao Y.Q., Shan J.G., He Z.G., Tian Y.T., Hu S.B., 2010b. Palaeogeothermal response and record of the effusing of Emeishan basalts in the Sichuan basin. Chin. Sci. Bull. 55(10), 949-956.

Zhu Y.M., Chen S.B., Fang J.H., Luo Y., 2010a. The geologic background of the Siluric shale-gas reservoiring in Szechwan, China. J. China Coal Soc. 35(7), 1160-1164.

Zhu Y.M., Hao F., Zou H.Y., Cai X.Y., Luo Y., 2007. Jurassic oils in the central Sichuan basin, southwest China: unusual biomarker distribution and possible origin. Org. Geochem. 38, 1884-1896.

Zou C.N., Yang Z., Dai J.X., Dong D.Z., Zhang B.M., Wang Y.M., Deng S.H., Huang J.L., Liu K.Y., Yang C., Wei G.Q., Pan S.Q., 2015. The characteristics and significance of conventional and unconventional Sinian-Silurian gas systems in the Sichuan Basin, central China. Mar. Pet. Geol. 64, 386-402.

Zou C.N., Yang Z., Pan S.Q., Chen Y.Y., Lin S.H., Huang J.L., Wu S.T., Dong D.Z., Wang S.F., Liang F., Sun S.S., Huang Y., Weng D.W., 2016. Shale Gas Formation and Occurrence in China: An Overview of the Current Status and Future Potential. Acta Geologica Sinica-English Edition. 90(4), 1249-1283.

Zou Y.R., Cai Y., Zhang C., Zhang X., Peng P., 2007. Variations of natural gas carbon isotope-type curves and their interpretation - a case study. Org. Geochem. 38, 1398-1415.

Zumberge J., Ferworn K., Brown S. 2012. Isotopic reversal (‘rollover’) in shale gases produced from the Mississippian Barnett and Fayetteville formations. Mar. Pet. Geol. 31, 43-52.

***Credit Author Statement**

Author contributions

Chunhui Cao: Conceptualization, Methodology, Investigation, Sample Analysis, Writing Original Draft, Project administration.

Mingjie Zhang: Supervision.

Liwu Li: Validation, Writing - Review & Editing, Supervision.

Yuhui Wang: Resources, Data Curation.

Zhongping Li: Resources, Data Curation.

Li Du: Resources, Data Curation.

***Declaration of Interest Statement**

Declaration of interests

☒ The authors declare that they have no known competing financial interests or personal relationships that could have appeared to influence the work reported in this paper.

☐The authors declare the following financial interests/personal relationships which may be considered as potential competing interests: